NUMEC P-90

PROGRESS REPORT

For Period October 1 through December 31, 1961
AEC R&D Contract AT(30-1)-2389

DEVELOPMENT
OF
PLUTONIUM-BEARING FUEL MATERIALS

NUMEC P-90

Nuclear Materials and Equipment Corporation
Apollo, Pennsylvania

~~For Official Use Only, Pending Patent Release~~

External Distribution List

U. S. Atomic Energy Commission, New York Operations Office
- M. Balicki
- H. S. Potter
- Leonard Topper
- Seymour Zirin

U. S. Atomic Energy Commission, Washington
- F. Charles Moesel (2)
- J. M. Simmons (5)
- M. Whitman
- M. Zeibold
- Reports and Statistics Branch

U. S. Atomic Energy Commission, Chicago Operations Office
- Bruce Anderson

U. S. Atomic Energy Commission, National Laboratories
- F. Foote, Argonne
- H. Young, Argonne (4)
- E. Childs, Dow Chemical
- E. A. Eschbach, Hanford
- E. A. Evans, Hanford
- W. K. Woods, Hanford
- O. J. Wick, Hanford
- J. Musser, Hanford
- I. D. Thomas, Hanford
- W. Cashin, KAPL
- H. Rizzo, Lawrence Radiation (3)
- R. D. Baker, Los Alamos
- L. B. Jones, Mound
- R. L. Mettler, Oak Ridge (3)
- D. F. Cope, Oak Ridge
- E. S. Bomar, Oak Ridge
- A. Squire, Westinghouse-Bettis

U. S. Atomic Energy Commission, Contractors
- W. J. O'Leary, Allis Chalmers Manufacturing Company
- R. W. Dayton, Bettelle
- W. Duckworth, Battelle
- G. M. Butler, Jr., Carborundum Company
- R. H. Gale, Combustion Engineering
- A. D. Schwope, Clevite Research Center
- L. A. Matheson, Dow Chemical Company
- G. Spaulding, Electric Autolite Company
- W. Alter, General Electric Company, Vallecitos
- L. D. Harris, National Carbon Company
- A. Strasser, Nuclear Development Corporation of America
- R. W. Hartwell, Power Reactor Development Company
- D. E. Hamby, Union Carbide Metals Company
- C. W. Kuhlman, United Nuclear Corporation
- Olin Mathieson Chemical Corporation

NUMEC Distribution List

R. J. Atkins
A. Biancheria
F. M. Cain
C. S. Caldwell
B. Cinai
J. Eck
G. Ehrlich
F. Forscher
R. Frumermann
H. J. Garber
E. E. Garcia
J. Goodman
O. S. Gray
E. K. Halteman
R. M. Horgos
R. A. Jaroszeski
L. J. Jones
W. Judd
A. Kasberg
H. Krake
A. L. Maharam
J. Marley
O. Menis
J. Miles
L. P. Pepkowitz
K. H. Puechl
P. Rey
J. E. Ross
W. G. Ross
J. Ruzbacki
J. Scott
Z. M. Shapiro
J. Stoner
M. M. Turkanis
B. Vondra
S. Weber
A. M. Weis
Library (5)

Previous Quarterly Progress Reports issued in this series are:

Number	For the Period Ending
NUMEC P-10	December 31, 1959
NUMEC P-20	March 31, 1960
NUMEC P-30	June 30, 1960
NUMEC P-40	September 30, 1960
NUMEC P-50	December 31, 1960
NUMEC P-60	March 31, 1961
NUMEC P-70	June 30, 1961
NUMEC P-80	September 30, 1961

TABLE OF CONTENTS

PROJECT AND FACILITY ADMINISTRATION

Task 1.00
K. H. Puechl

Summary of Development Activities

During this reporting period, continued strong effort has been placed on the preparation and characterization of PuO_2 and UO_2-PuO_2 mixtures. Sintering trials and characterization of pellets have also been given emphasis, since this fabrication route will be used for the initial irradition test samples. Effort has also continued on plasma torch production of spherical PuO_2 particles as well as the metallic coating of oxide materials. Reactor physics studies have been continued in order to determine the effect of cross section assumptions on the calculated behavior of plutonium-fueled near-thermal reactor systems.

PuO_2 has been prepared via the oxalate process using dilute plutonium nitrate starting solutions in order to obtain information relative to internal recycling of plutonium-contained materials. The resulting PuO_2 powders have been analyzed to determine their characteristics relative to the powders normally produced. It has been found that the PuO_2 produced from the low plutonium concentration feed contains agglomerates that are not readily broken down; in comparison, PuO_2 produced from normal feed concentration contains larger agglomerates, but these are readily dispersed ultrasonically. In addition, it has been found that the surface area of material produced from the low concentration feed is less sensitive to the hold time at temperature during calcination.

The water titration method for determining the total porosity of powders has now been satisfactorily adapted for use with PuO_2. Porosity determinations have been made on various samples of materials produced in the past.

A study of the moisture pickup of PuO_2 powders during storage has been completed. Equilibrium moisture content for various humidities has been determined as a function of the powder calcination temperature (surface area). It has been concluded that for most ceramic powders of interest, the moisture pickup problem with PuO_2 will not be significantly different from that encountered in the handling of ceramic-grade UO_2.

Thermogravimetric studies performed on plutonium oxalate powders that had been stored for various periods of time indicate that plutonium oxide decomposes at room temperature. Evidence of this decomposition has also been verified by x-ray examination. It is postulated that this room temperature decomposition is probably due to alpha radiolysis or localized alpha decay heat.

Particle surface areas have been measured at various stages during thermal decomposition of plutonium oxalate. A sudden rise in surface area has been noted, starting at about 275°C; it is concluded that this rise in surface area is due to a breakdown in the crystallite structure caused by fissures that occurred during escape of decomposition gases.

A number of essentially production runs were carried out on UO_2-PuO_2 mixtures in order to determine the degree of reproducibility. A total of thirteen 600 gm lots were prepared for the three compositions UO_2-0.5 w/o PuO_2, UO_2-5.0 w/o PuO_2, and UO_2-20 w/o PuO_2. Samples of each lot were subjected to various physical and chemical tests, including composition assay, trace analysis, oxygen/uranium ratio, surface area, and particle size. These results indicate that reproducibility was satisfactory.

Several prototype lab-scale experiments have been carried out on UO_2 in order to determine the feasibility of preparing directly dense, coarse UO_2-PuO_2 and PuO_2 powders for use as feed for the plasma torch, mechanical packing, and swaging. The preparation routes examined include homogeneous precipitation employing uranyl nitrate hexahydrate (UNH) and urea, uranyl sulfate and urea, and UNH and ammonium carbonate. The characteristics of the resultant UO_2 products appear to be sufficiently interesting to warrant extension of this work to PuO_2.

Development of analytical chemistry techniques for use with plutonium and plutonium-uranium mixtures has been continued. A procedure for the potentiometric titration of plutonium that is more rapid than the previously developed amperometric method has been satisfactorily utilized. In addition, studies have been initiated on the polarographic determination of oxygen-to-metal ratios in plutonium-uranium oxide mixtures. X-ray fluorescence and gamma counting procedures have also been developed for assaying low-level plutonium residues. Preliminary studies have been carried out on alpha ray spectrometry on plutonium and other transuranium elements.

During the fabrication of UO_2-5 w/o PuO_2 pellets by the cold press and sintered procedure, two phenomena relating to the firing process were observed. One phenomenon was fracturing of the sintered pellets and the other was the appearance of a glassy coating on some pellet surfaces. These two effects may be interrelated and will be further investigated. Other sintering studies were performed to determine the possibility of re-using fired pellet material as a portion of the pre-pressed powder mix. The results indicate that this procedure is not satisfactory; a number of oxidation-reduction cycles, as used in the recycling of UO_2, are probably necessary.

The two-phase eutectoid microstructure observed in PuO_2 pellets after sintering in a nitrogen-6% hydrogen atmosphere has now been positively identified as PuO_2 and cubic Pu_2O_3. Assuming that the PuO_2 and Pu_2O_3 in the eutectoid were formed from a single stable phase at the sintering temperature, the composition of the latter was calculated to be $PuO_{1.873}$. Differential thermal analysis indicates that the eutectoid transformation probably occurs between 600-700°C. The roll of residual carbon in the decomposition and fusion of the PuO_2 has also been investigated further. It has been concluded that the carbon is primarily responsible for the observed fusion, probably due to the formation of an oxycarbide of plutonium similar to that observed in the U-O-C system. Experiments indicate, however, that the carbon is probably not responsible for the conversion of PuO_2 to Pu_2O_3.

Fabrication of rabbit test capsules for irradiation studies are now in progress. The objective of these experiments will be to determine the "thermal performance" of UO_2-PuO_2 mixtures relative to a UO_2 standard sample. Initial capsules will be fabricated by the sintered pellet-in-tube technique and will allow comparison between co-precipitated and mechanically-mixed UO_2-PuO_2 powders.

Spherical PuO_2 particles have now been produced with the plasma torch. Good size and sphericity control was achieved using either crushed high-fired pellets or pre-formed high-fired particles as feed material. Spherical particles can be produced by total melting within the torch or by melting just the surface. When total melting occurs, most particles contain a central void.

Spherical particles of PuO_2 have also been prepared by the use of a multi-step process of drying, pressing, granulation, sizing, shaping, and sintering. In general, these particles are not as spherical as those produced with the plasma torch, and they do not have the glassy fire-polished finish. These particles have been successfully coated with an "electroless" nickel coating up to 20 microns in thickness, and an electrolytic copper coating up to 15 microns in thickness applied over a 2-4 micron "electroless" nickel base coat. Electrolytic copper has also been applied over a vacuum evaporated 1-3 micron copper base coat; this coating did not appear to be satisfactory, however.

Reactor physics studies on near-thermal plutonium-fueled systems have been continued to determine the sensitivity of the results to changes in the effective cross sections of the various isotopes. These studies were initiated in order to verify the optimistic conclusions with regard to plutonium utilization arrived at previously. Results to date generally verify the initial conclusions. More of the materials development effort will, therefore, be directed in the directions indicated by these studies. Two papers having the titles "The Potential of Plutonium as a Fuel in Near-Thermal Converter Reactors" and "The Potential of Plutonium as a Fuel in Near-Thermal Burner Reactors" which cover the initial physics work on these systems will be published in the February 1962 issue of Nuclear Science and Engineering.

General Plant Operations

Two more glove boxes have been completely outfitted and have passed leak-testing specifications. These are the corrosion test box (which also includes an area for electron microscope sample replication) and the decontamination box. In addition, the welding box is in the final stages of outfitting, and work has started on equipment installation in the alpha boxes required for post-irradiation examination.

The causes of the previous sintering furnace failures have been ascertained. In one case, a low melting impurity had accidentally been in contact with the molybdenum windings. In the other case, two adjacent windings were in contact, causing a localized hot spot and melting of the alumina muffle. Both furnaces have been reactivated during this quarter, and they have been operating satisfactorily.

Since the last report period, 33 additional gloves have failed and have been successfully changed without any evidence of alpha contamination external to the glove boxes. Glove-changing is now a completely routine operation.

PREPARATION AND CHARACTERIZATION OF FUEL MATERIALS

Task 2.00

C. S. Caldwell O. Menis

Plutonium Oxide Preparation via Oxalate Process and Resultant Powder Characterization

(C. S. Caldwell, R. J. Atkins, A. Biancheria, G. Ehrlich, J. Goodman, H. Krake)

During this reporting period, PuO_2 was prepared via the oxalate process using dilute plutonium nitrate starting solutions in order to obtain information relative to internal recycling of plutonium-contained materials. The resulting PuO_2 powders were analyzed to determine their characteristics relative to those of powders normally produced. In addition, characterization of previously produced powders was continued. Also, the simple method for determining total porosity previously described has now been extended to PuO_2 samples.

Studies have also been continued in order to give a better understanding of the oxalate process. Specifically, weight pickup during storage of PuO_2 powders has been investigated. Further, thermogravimetric studies have been carried out to study the oxalate decomposition, and variations in particle surface area and size have been measured at a number of stages during oxalate thermal decomposition.

Preparation of PuO_2 via Oxalate Process

Preparation of PuO_2 via the oxalate process from dilute plutonium nitrate starting solutions has yielded information of interest for the processing of plutonium recycle streams where no intermediate concentrating step is planned. Processing conditions for two continuous runs and one batch run are summarized in Table 2.1.

PuO_2 Powder Characterization

Characterization of previously produced PuO_2 powder, designated 297-Pu-9, Lots I, II, III and IV(i) has been continued. Similar characteristics have also been measured on materials produced from low plutonium concentration feed (Samples 297-Pu-11A, 11B, and 12B; see Table 2.1). The resulting characterization data are shown in Table 2.2.

(i) NUMEC P-80, Progress Report, "Development of Plutonium-Bearing Fuel Materials", page 10.

Table 2.1

Summary of Process Conditions Used During Preparation of PuO_2 from Dilute Plutonium Nitrate Solutions

Sample Identification	297-Pu-11A	297-Pu-11B	297-Pu-12B
Precipitation Conditions			
Method	Continuous	Continuous	Batch
Temperature, °C	35	35	55
Feed Composition, gm Pu/liter	20	12	10.5
H^+, Molarity	3	3	3
Strike Solution Composition			
$H_2C_2O_4$, Molarity	1.0	1.0	1.0
H_2O_2, Molarity	0.8	0.8	0.8
Precipitation Average Holdup, minutes	23	20	-
Total Number Throughputs	15.5	24.2	-
Drying Temperature, °C	180	180	180
Furnace Conversion Conditions			
Temperature, °C	760	760	350
Time, minutes	30	30	15

Table 2.2

Powder Characteristics of Various PuO_2 Samples

Sample	Feed Composition gm Pu/liter	Calcination		Bulk Density gm/cc	Tap Density gm/cc	Air Permeability Avg. Diameter, microns	B.E.T. Surface Area M^2/gm	M.S.A. 50% Particle Size microns	
		Temp °C	Time min					Dispersed in Burrell Shaker	Dispersed in Ultrasonic Field
297-Pu-9-Lot 1	100	760	30	1.97	2.62	2.42	3.4	5.4	3.1
297-Pu-9-Lot 2	100	760	30	1.76	2.30	2.57	5.4	10.1	3.2
297-Pu-9-Lot 3	100	350	30	1.01	1.25	1.63	43	10.6	4.6
		+760	30				4.1		
297-Pu-9-Lot 4	100	760	17	2.09	2.31	3.55	7.5	9.4	2.4
297-Pu-11A	20	760	30	2.26	2.80	2.58	8.3	5.2	5.0
		+760	30				6.1		
297-Pu-11B	12.5	760	30	2.26	2.74	2.28	7.15	5.7	4.6
297-Pu-12B	10.5	350	15	1.75	2.14	2.70	52		

A comparison of the measured surface areas for samples 9-Lot I and Lot II (held for 30 minutes at 760°C) with Lot IV (held for 17 minutes at 760°C) indicates that the surface area for this material derived from a 100 gm/liter feed solution is sensitive to the hold time at a calcination temperature of 760°C. Specifically, the surface area 7.5 M^2/gm at a hold time of 17 minutes decreases to 3.4-5.4 M^2/gm at a hold time of 30 minutes. This sensitivity is substantiated by all pertinent data obtained earlier and reported in previous progress reports. In comparison, the surface area of PuO_2 produced from low concentration feed solution seems to be less sensitive to hold time at 760°C. Specifically, the powder from Sample 11A held for 30 minutes at 760°C was found to have a surface area of 8.3 M^2/gm, while after re-calcination at the same temperature for an additional 30 minutes the surface area remained quite high at 6.1 M^2/gm.

The particle size data obtained with the Mine Safety centrifuge also show another difference between powders prepared from different plutonium concentrations in the feed solution. More complete data than presented in Table 2.2 are shown in Figures 2.1 and 2.2. These data show that the powders prepared from the 100 gm/liter feed solutions contain larger agglomerates but that these are more readily broken down than those prepared from the more dilute feed. The relatively large particle size associated with the low feed concentration product even after ultrasonic dispersion may be an indication of possible poor reproducibility in subsequent fabrication operations.

From the results shown in Table 2.2 and those reported previously on powders prepared from normal (100 gm/liter) feed concentration, one can deduce an average variation of surface area with hold time at 760°C. This is shown in Figure 2.3. It is seen that over the range of 5 to 30 minutes hold time, the surface area decreases in essentially a linear fashion.

The water titration method for determining the total porosity of powders as previously described(i) has now been adapted for use with PuO_2. Porosity determinations on three samples (297-Pu-9-Lot III, 297-Pu-4 and 297-Pu-5) have been made. Excellent reproducibility was obtained. The results on Sample 9-Lot III are shown as a function of hold time at 760°C in Figure 2.3. It is seen thereon that the porosity variation with hold time is similar to the associated variation in surface area. Results on the other two samples are presented in Figure 2.4 as a function of the calcination temperature. It is seen that the total porosity rises with calcination temperature to 560°C and then drops off rapidly. This variation is appreciably different from the associated variation in surface area which had previously been shown to remain nearly constant to 490°C and then fall of linearly(ii).

(i) NUMEC P-80, Progress Report, "Development of Plutonium-Bearing Fuel Materials", pages 22.

(ii) NUMEC P-80, Progress Report, "Development of Plutonium-Bearing Fuel Materials", page 14.

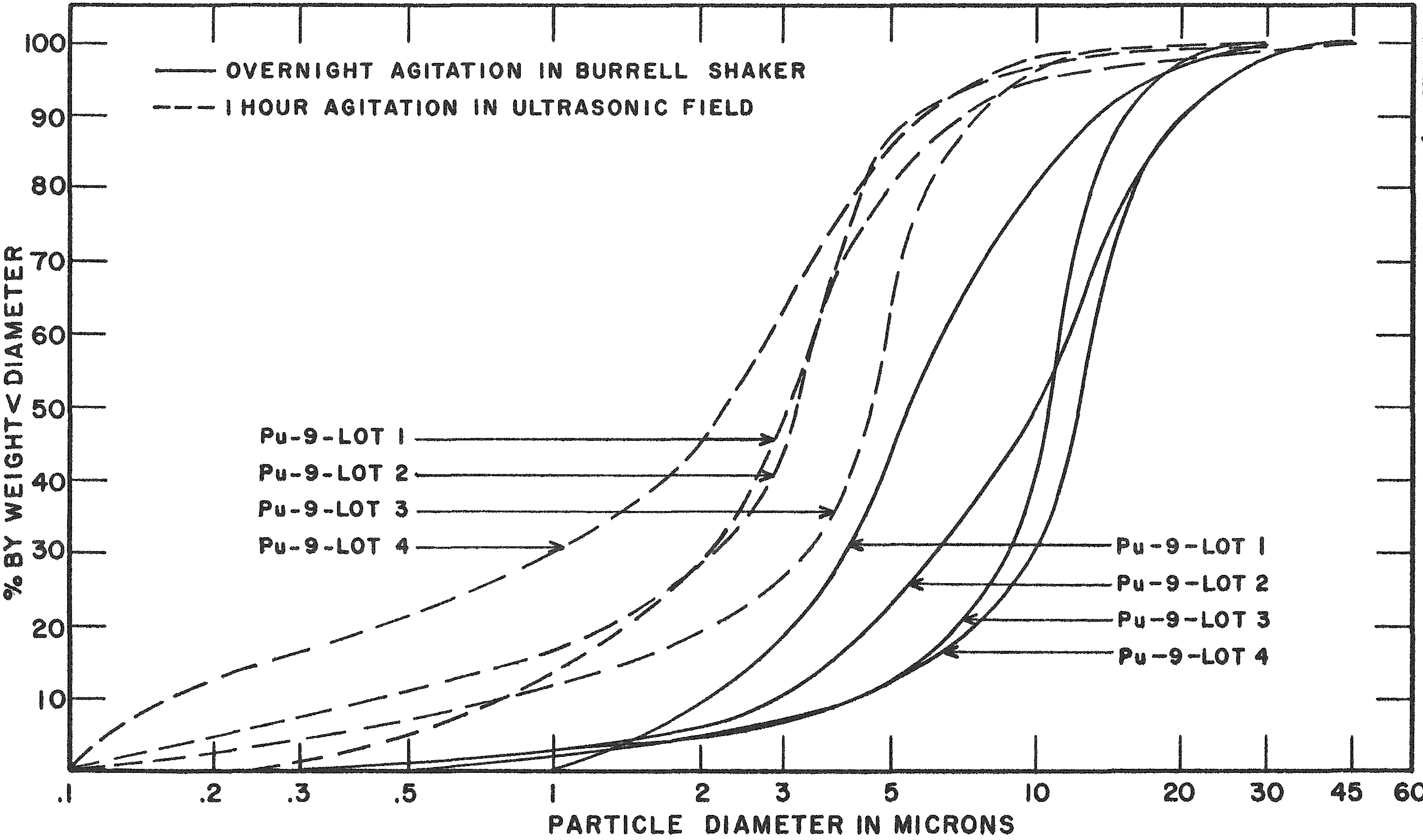

Figure - 2.1

EFFECT OF DISPERSION METHOD ON PARTICLE SIZE DISTRIBUTION
OF
PLUTONIUM DIOXIDE SAMPLES Pu-9-LOTS 1-4

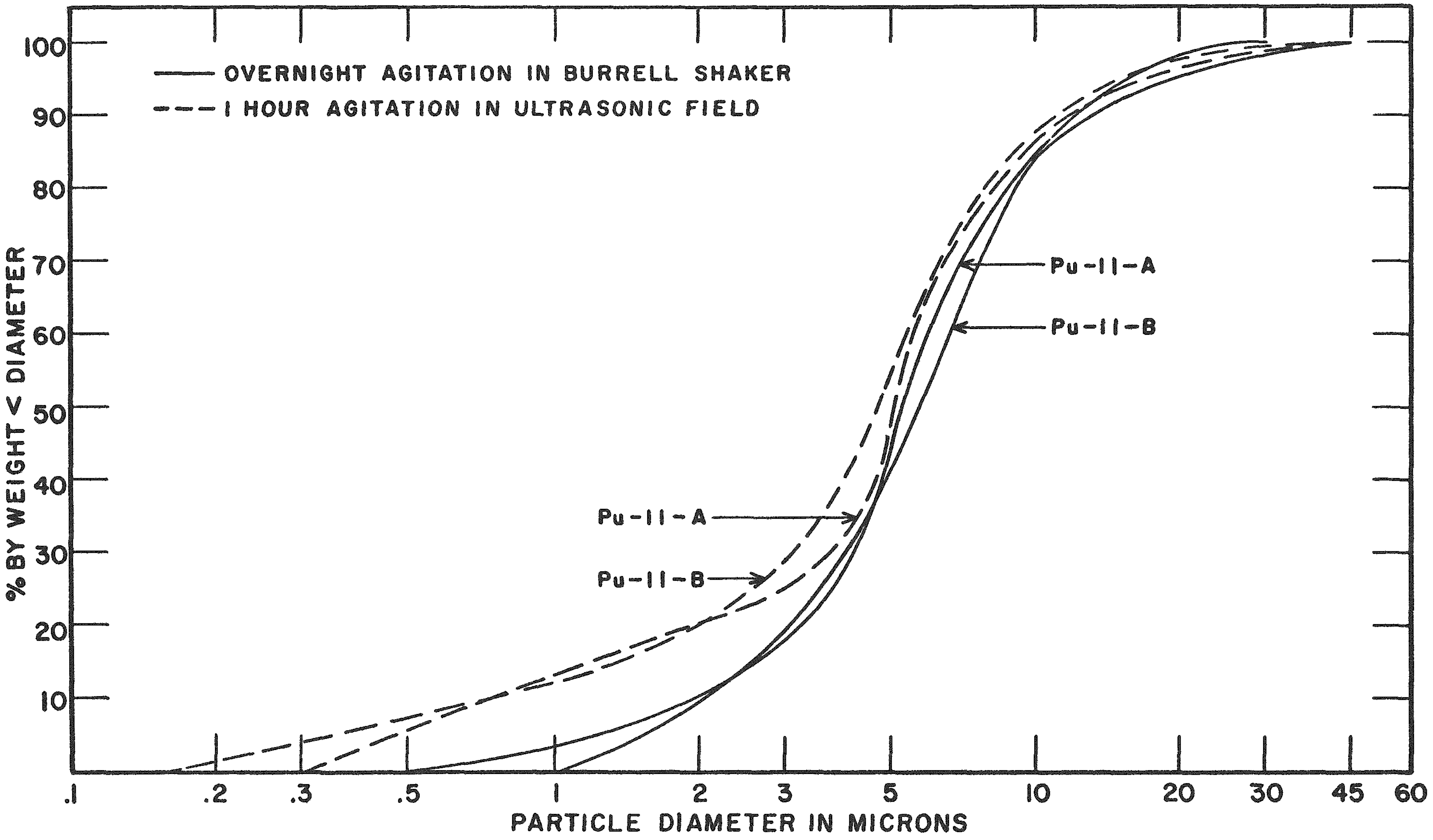

Figure-2.2

EFFECT OF DISPERSION METHOD ON PARTICLE SIZE DISTRIBUTION
OF
PLUTONIUM DIOXIDE SAMPLES 11A and 11B

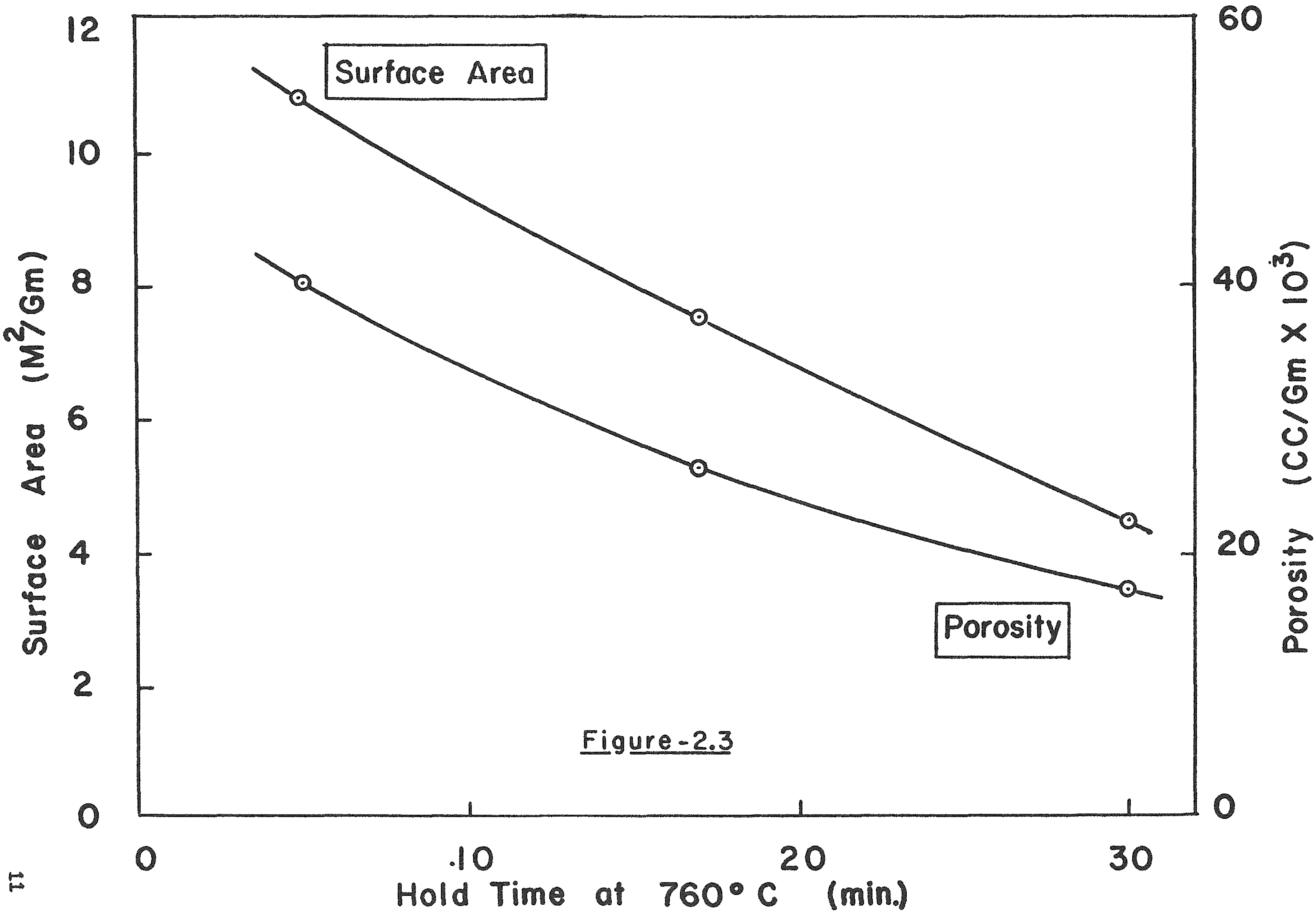

Figure-2.3

EFFECT OF HEAT TREATMENT ON PuO_2 PROPERTIES

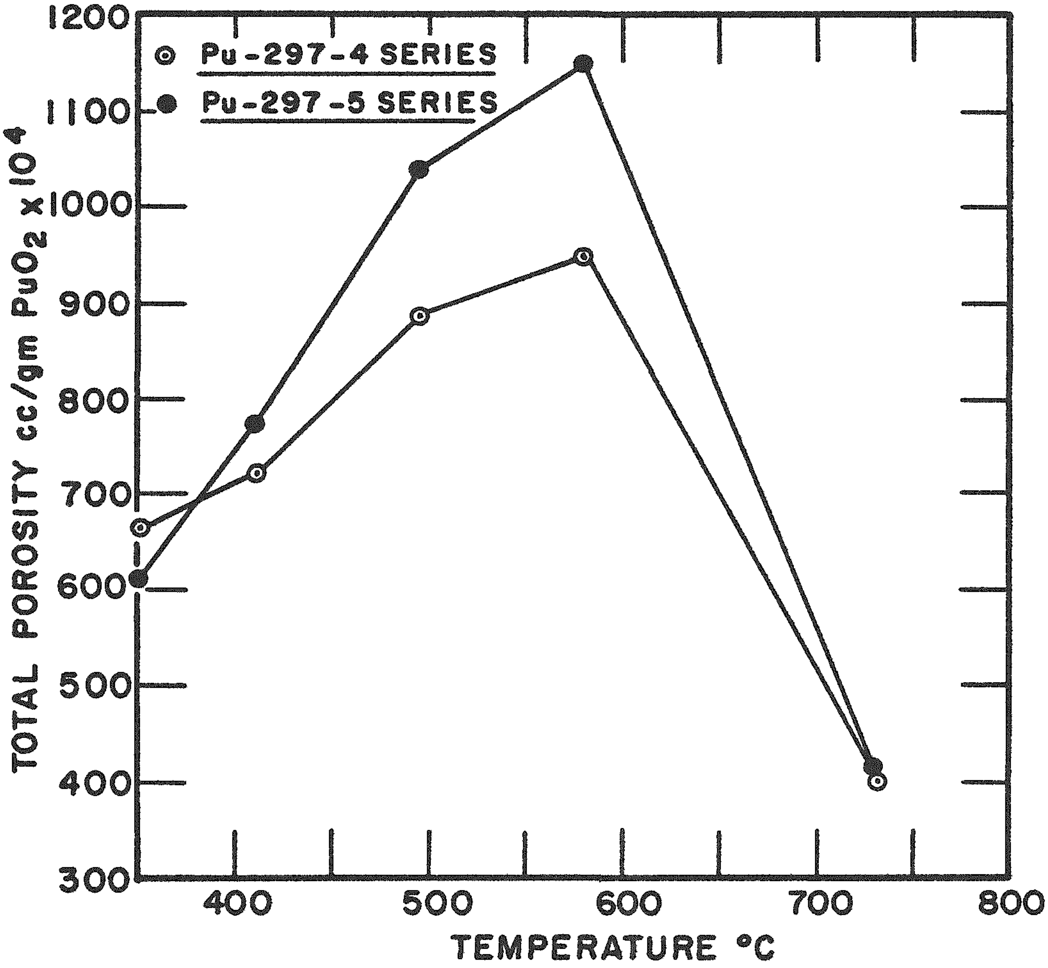

Figure-2.4

EFFECT OF CALCINATION TEMPERATURE ON TOTAL POROSITY OF PLUTONIUM DIOXIDE POWDER

In our early experimental work with PuO_2 powders of high surface area, it was noticed that large changes in sample weight occurred during storage, and it was suspected that most, if not all, of this effect was due to moisture absorption from the ambient air(i). In order to establish the limits of moisture pickup to be expected with PuO_2 powders of different surface area under various environmental humidity conditions, a series of carefully-dried powder samples were exposed to controlled conditions in the range of 33 to 97% relative humidity at room temperature for periods up to 300 hours.

For these experiments, 297-Pu-4 powders were utilized. Preparation and characterization data for these materials have been presented in previous Quarterly Progress Reports.

Three sets of PuO_2 powder samples calcined at 350, 490, and 760°C were dried to constant weight and placed in constant humidity chambers. Relative humidities of 33, 53, 76, and 97% were obtained by the use of saturated solutions of $MgCl_2 \cdot 6H_2O$, $Mg(NO_3)_2 \cdot 6H_2O$, NaCl, and K_2SO_4, respectively.

The associated weight gain data as a function of time are presented in Figures 2.5-2.8. In the humidity range between 33 and 76%, 90% of the equilibrium moisture was picked up within 6 to 12 hours. At 97% relative humidity, the samples continued to gain weight up to 100 hours, with 90% of equilibrium being attained, in most cases, within 50 hours. The unexpected weight decreases observed at 97% relative humidity (Figure 2.6) after 115 hours exposure are being checked by repeating the measurements at several points.

The equilibrium moisture contents as a function of relative humidity are shown in Figure 2.9; the strong effect of calcination history is illustrated. Within the mid-range of humidity (33-53%), the equilibrium moisture content of the powder prepared by calcination at 760°C is relatively insensitive to humidity; an equilibrium moisture level of 0.1 to 0.15% was obtained in this range. Since the powder has a surface area of 10-12 M^2/gm(ii), and considering that the surface areas of most powders to be used in ceramic fuel fabrication will probably fall below this range, the PuO_2 moisture pickup problem is expected to be not appreciably different from that encountered in the handling of ceramic-grade UO_2.

The variation of the equilibrium moisture content with powder calcination temperature is shown in Figure 2.10. A nearly linear relationship is illustrated in the low to medium relative humidity range. In this humidity

---

(i) NUMEC P-60, Progress Report, "Development of Plutonium-Bearing Fuel Materials", page 22.

(ii) NUMEC P-80, Progress Report, "Development of Plutonium-Bearing Fuel Materials", page 12.

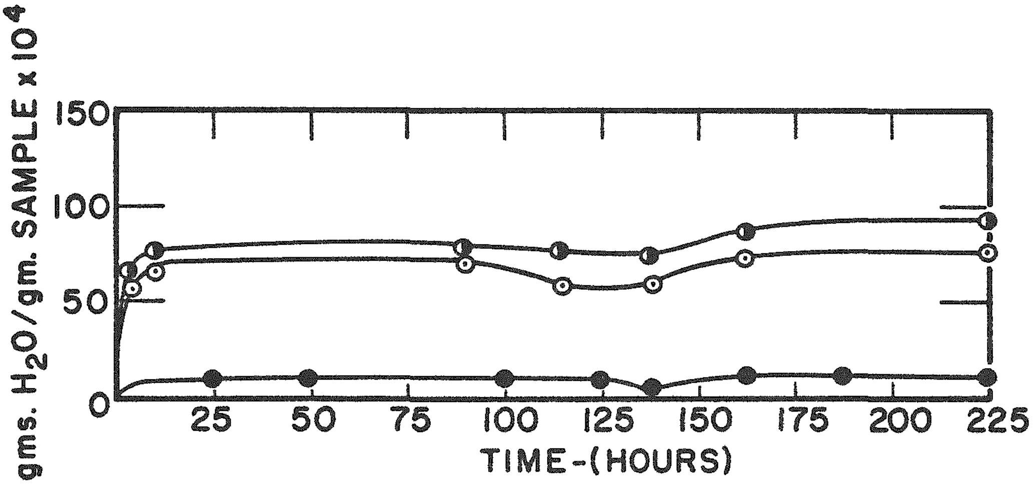

Figure - 2.5

WATER ABSORPTION IN PuO_2 AT 33% RELATIVE HUMIDTY

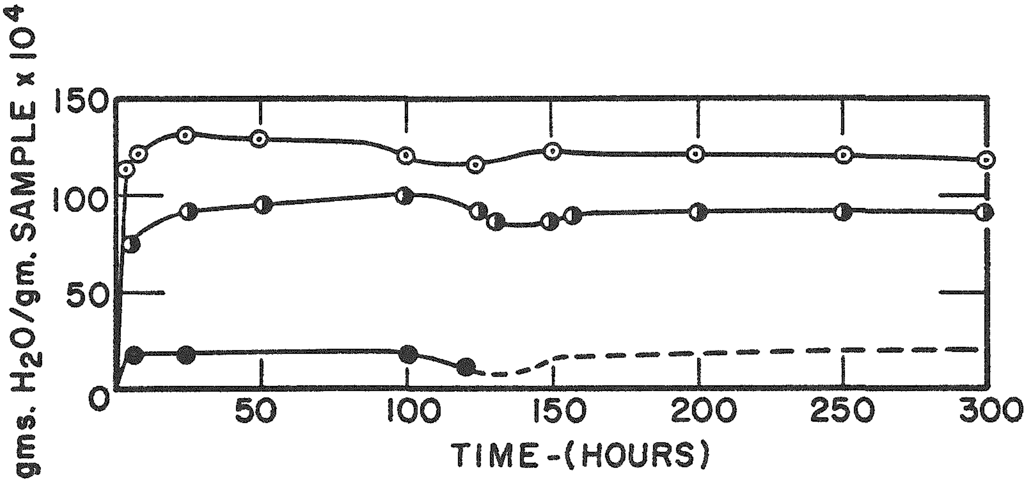

Figure - 2.6

WATER ABSORPTION IN PuO_2 AT 53% RELATIVE HUMIDITY

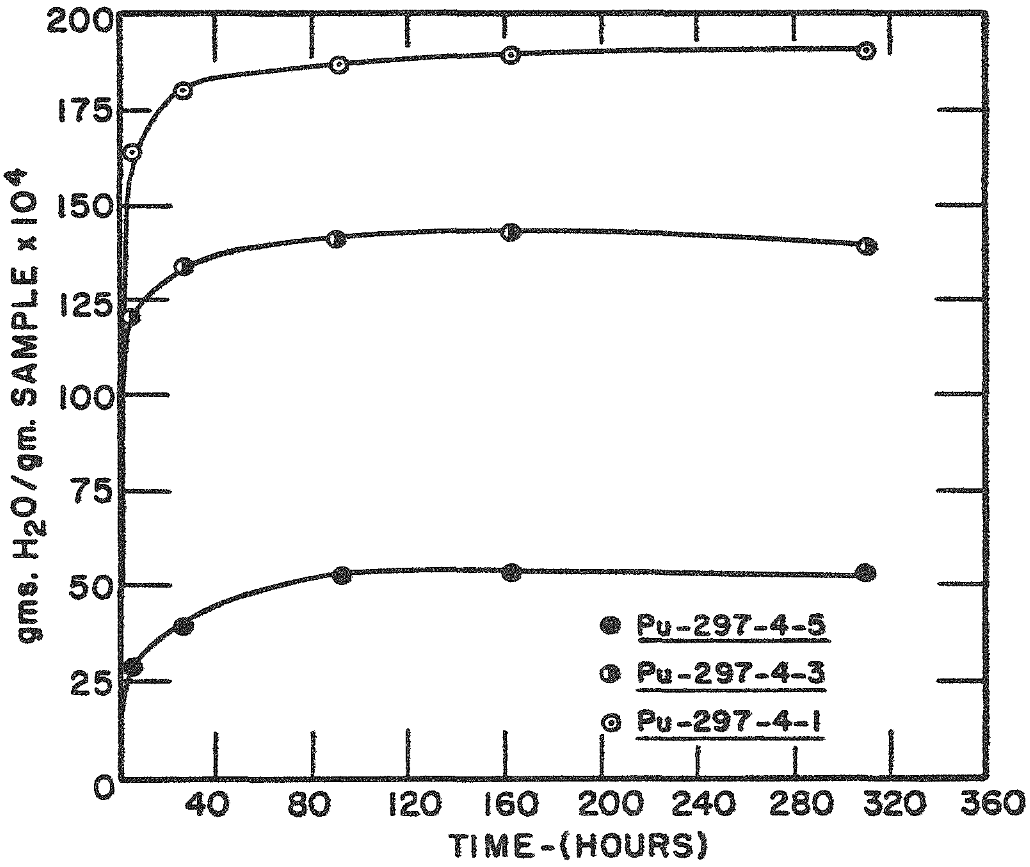

Figure-2.7

WATER ABSORPTION IN PuO_2
AT 76% RELATIVE HUMIDITY

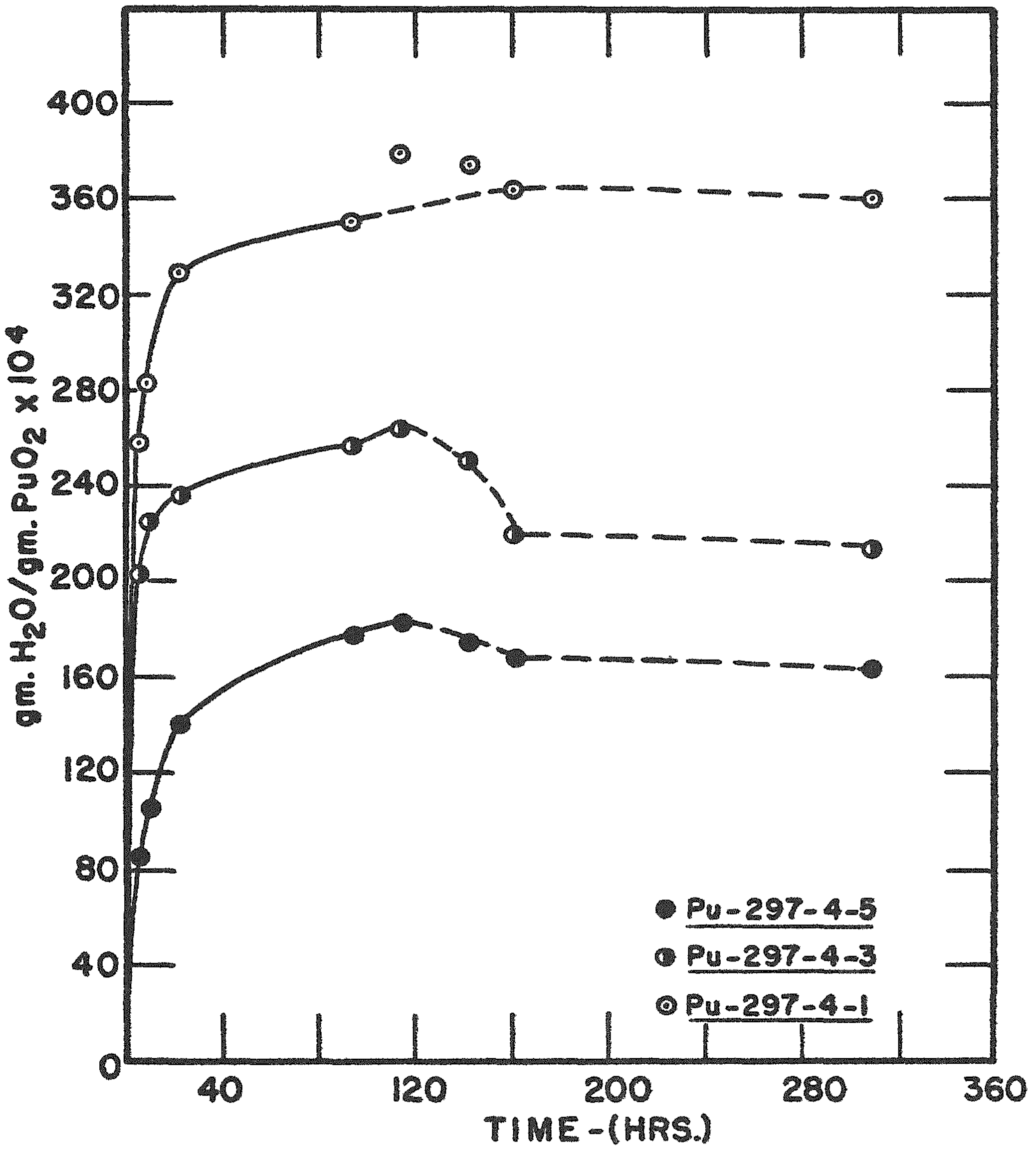

Figure-2.8

WATER ABSORPTION IN PuO_2 AT 97% RELATIVE HUMIDITY

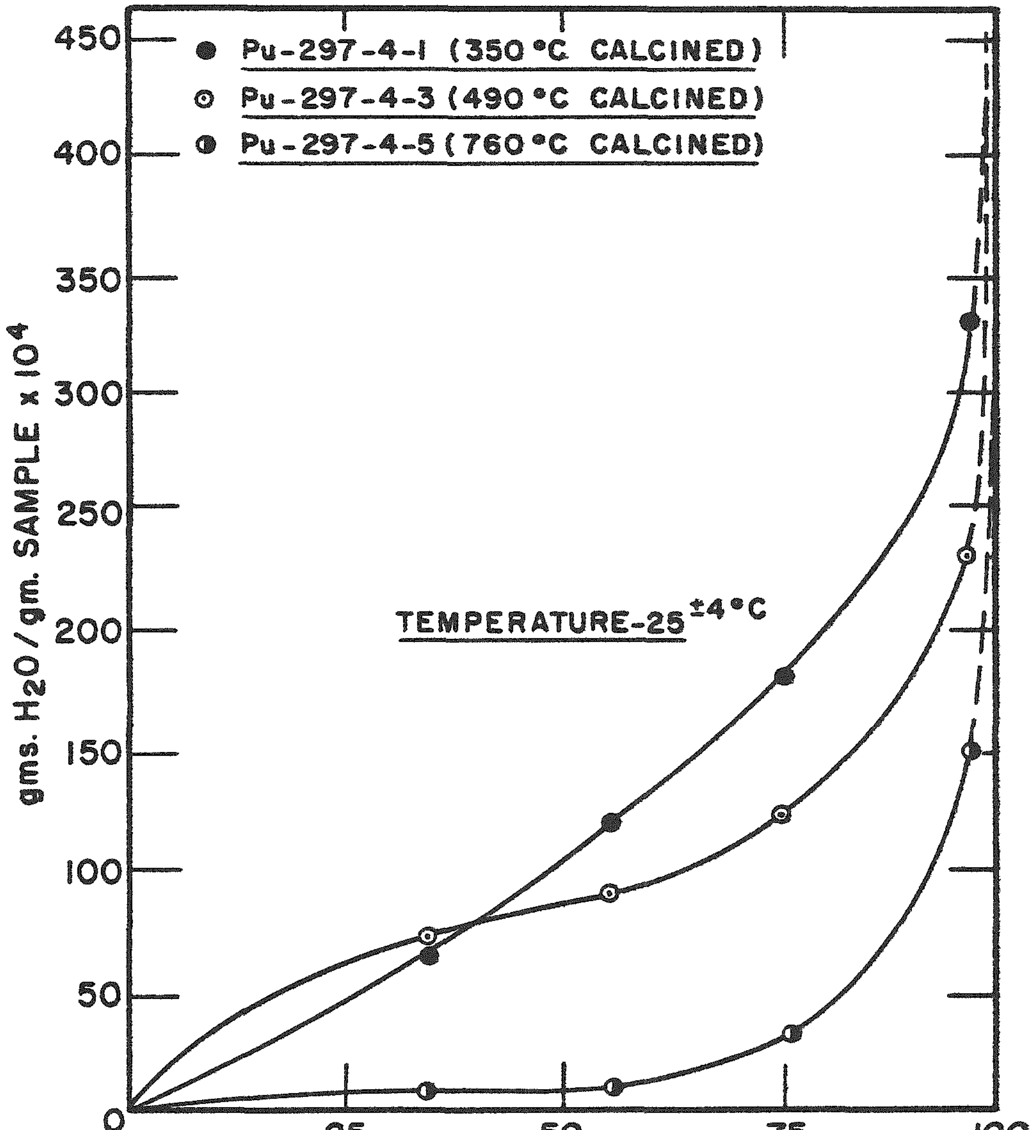

Figure-2.9

EQUILIBRIUM MOISTURE CONTENT OF PuO_2 V.S. AMBIENT HUMIDITY

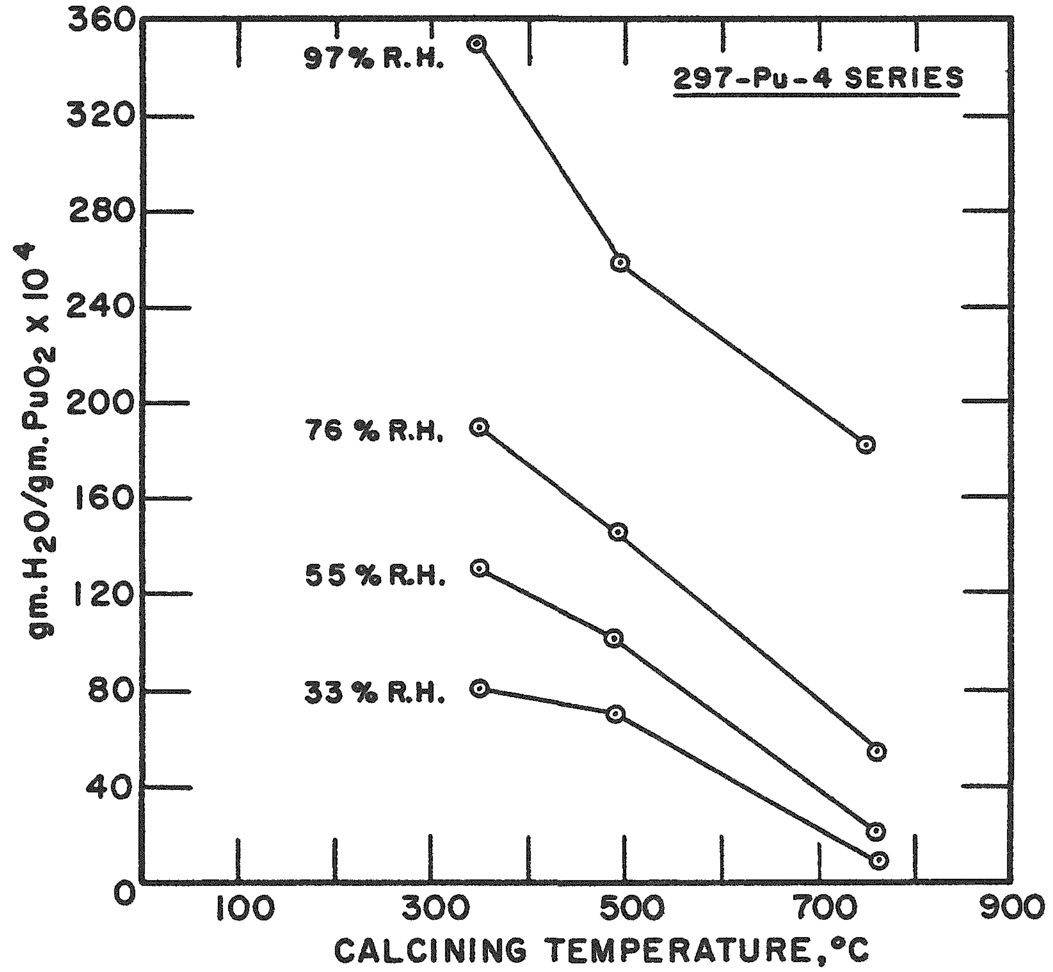

Figure - 2.10

EFFECT OF CALCINATION TEMPERATURE ON EQUILIBRIUM MOISTURE CONTENT OF PuO_2 POWDER range. the equilibrium moisture content seems to vary directly as the powder surface area; i.e., the surface area decreases by about a factor of 5 over the calcination temperature range 350 to 760°C, and the equilibrium moisture content likewise decreases by roughly the same magnitude. In the high humidity range where condensation effects in large capillaries can be expected, the variation in equilibrium moisture content with powder calcination temperature is somewhat less pronounced.

Thermogravimetric Studies on the Decomposition of Plutonium Oxalate

Thermogravimetric studies on the decomposition of plutonium oxalate, $Pu(C_2O_4)_2$, have been continued to gain further understanding of the process chemistry and to aid in the optimization of processing conditions. The results obtained during this reporting period are shown in Figures 2.11 through 2.14. In all cases a heating rate of 6°C/min and a flow rate of 2 SCFH were employed.

Previous data(i) indicated that a gradual decomposition of the oxalate seems to occur during storage at room temperature. This postulated decomposition was further investigated by performing thermogravimetric analyses on identical samples after varying storage periods. Figure 2.11 shows a comparison of the decomposition curves obtained in air on two different days using Sample 297-Pu-Ox-9-Lot I. The curves dated 10-9-61 shows a definite decomposition stage between 150 and 250°C (the initial weight decrease between 50 and 130°C was assumed to be due to loss of water) and the weight after drying, taken at 150°C when compared to the final PuO_2 weight indicates that the oxalate was 5% decomposed. On the other hand, the curve dated 10-27-61 does not show a definite decomposition stage in this temperature range and the weight after drying indicates that the oxalate was 17% decomposed. Similar results were obtained in a nitrogen atmosphere. Specifically in Figure 2.12 are shown the data obtained on 10-20-61. This curve does not show the low temperature decomposition stage reported previously(ii) for the same material analyzed earlier. Analysis of the later measurements indicates that the oxalate was 15% decomposed after drying. This is in essential agreement with the results obtained in air. Data on two samples of freshly-formed oxalate were also obtained in order to determine if the weight loss after drying is consistent with the formula $Pu(C_2O_4)_2$. These data are shown in Figures 2.13 and 2.14. The results indicate that anhydrous $Pu(C_2O_4)_2$ is indeed the stable compound formed after the drying period; agreement with this interpretation is within 0.3% for Sample 297-Pu-OX 11A and within 1.7% for Sample 297-Pu-OX-12B.

(i) NUMEC P-80, Progress Report. "Development of Plutonium-Bearing Fuel Materials", page 15.

(ii) NUMEC P-80 Progress Report "Development of Plutonium-Bearing Fuel Materials". page 17.

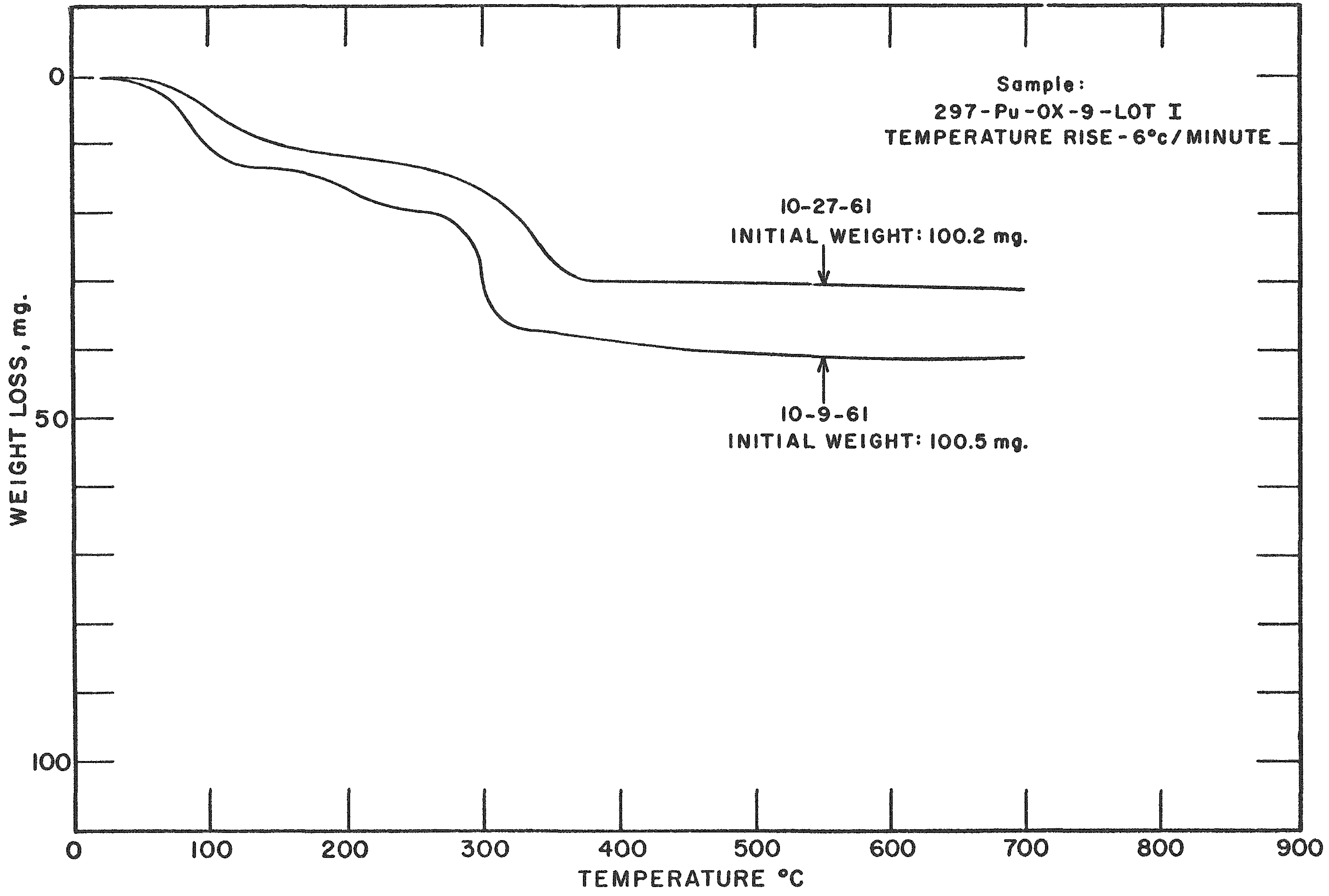

Figure-2.11

THERMOGRAVIMETRIC DECOMPOSITION CURVE

AIR ATMOSPHERE

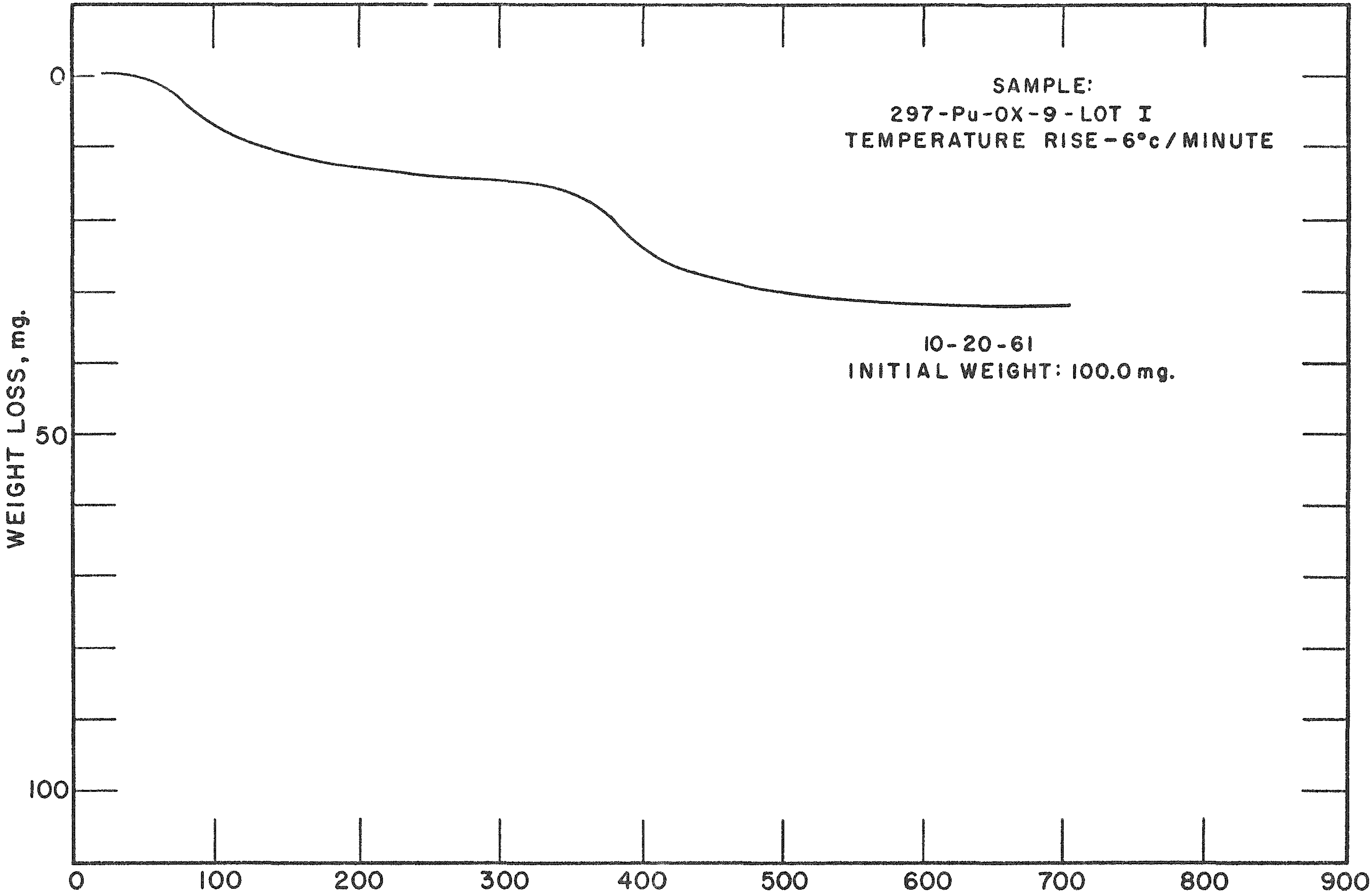

Figure-2.12

THERMOGRAVIMETRIC DECOMPOSITION CURVE
NITROGEN ATMOSPHERE

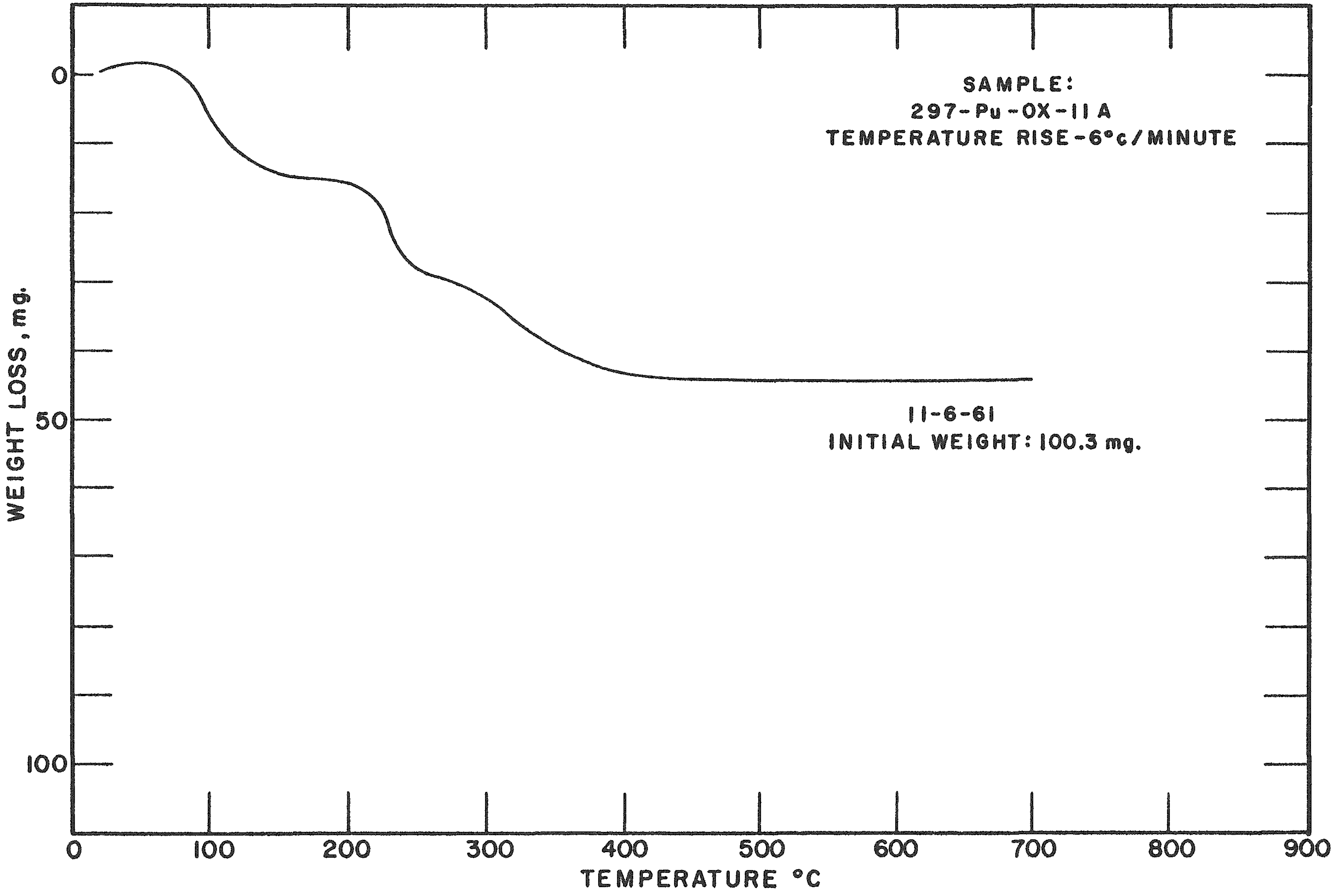

SAMPLE:
297-Pu-OX-11 A
TEMPERATURE RISE-6°c/MINUTE

11-6-61
INITIAL WEIGHT: 100.3 mg.

Figure-2.13

THERMOGRAVIMETRIC DECOMPOSITION CURVE
AIR ATMOSPHERE

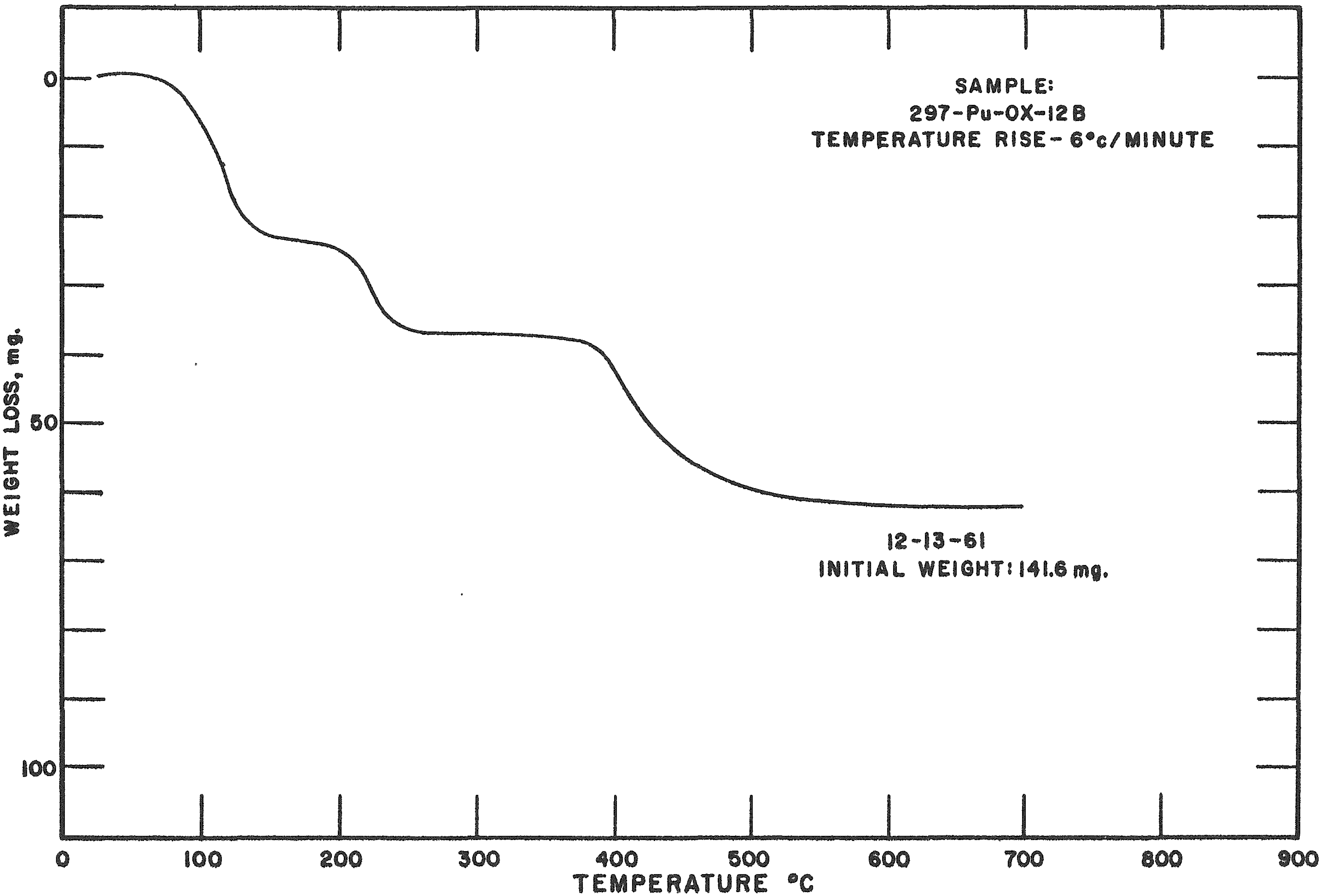

SAMPLE:
297-Pu-OX-12B
TEMPERATURE RISE - 6°c/MINUTE

12-13-61
INITIAL WEIGHT: 141.6 mg.

Figure-2.14

THERMOGRAVIMETRIC DECOMPOSITION CURVE

NITROGEN ATMOSPHERE

Further evidence that decomposition occurs at room temperature was obtained by x-ray examination. Faint but definite PuO_2 lines were observed on 10-20-61 in the diffraction pattern for an aged Sample 297-Pu-OX-9-Lot I showing that some complete degradation had occurred. For the fresh oxalate samples, 297-Pu-OX-11A and 12B, no PuO_2 was detected. When re-examined at a later date (46 days later for 11A and 21 days later for 12B), the presence of PuO_2 still could not be observed, but the "oxalate" diffraction lines were now much more diffused, and some of the fainter lines had disappeared. These samples will be re-examined periodically to determine if any further changes are occurring.

This room temperature decomposition is attributed to α-radiolysis or localized α-decay heat. Chemical instability, as such at room temperature does not appear plausible in view of the fact that PuO_2 lines were detected in the x-ray pattern of an unheated sample while the thermogravimetric data on freshly-formed oxalate (Figures 2.13 and 2.14) show the formation of a stable intermediate.

The available data is not sufficient to assign a definite mode of decomposition for plutonium oxalate However, the two stage reaction (after drying) for the fresh oxalate samples strongly suggest that the reactions $Pu(C_2O_4)_2 \longrightarrow Pu(CO_3)_2 + 2CO\uparrow$ and $Pu(CO_3)_2 \longrightarrow PuO_2 + 2CO_2\uparrow$ play a major role. Analysis on this basis yielded for Sample 11A, Figure 2.13, an observed CO loss of 14 mg compared to a calculated value of 11.4 mg and an observed CO_2 loss of 15 mg compared to a calculated value of 17.9 mg. Sample 12-B Figure 2.14, yielded an observed CO loss of 13 mg compared to a calculated value of 15.9 mg and an observed CO_2 loss of 26 mg compared to a calculated value of 25 mg. While this constitutes fair agreement, further confirmation, such as the analysis of the off gases, is required in order to assign a definite decomposition route.

Surface Area and Particle Size Changes During Thermal Decomposition of Plutonium Oxalate

In order to investigate the origin of the high surface areas observed for several PuO_2 samples, surface area measurements have been carried out on plutonium oxalate samples during various stages of thermal decomposition. Results on Sample 297-Pu-OX-9-Lot II were reported earlier(i). At 275°C these data showed a sudden rise in total available surface area. To confirm this trend, measurements were repeated using Sample 297-Pu-OX-11A prepared from dilute plutonium nitrate feed. The resulting surface areas based on the weight of the final PuO_2 powder are shown in Figure 2.15 as a function of the calcination temperature. It is to be noted that the variation of available surface area with calcination temperature is similar to that obtained previously. Evidence that this variation also occurs in the conversion of ADU to UO_2 has been obtained in other related studies reported in a later section of this report.

(i) NUMEC P-80, Progress Report, "Development of Plutonium-Bearing Fuel Materials" page 16.

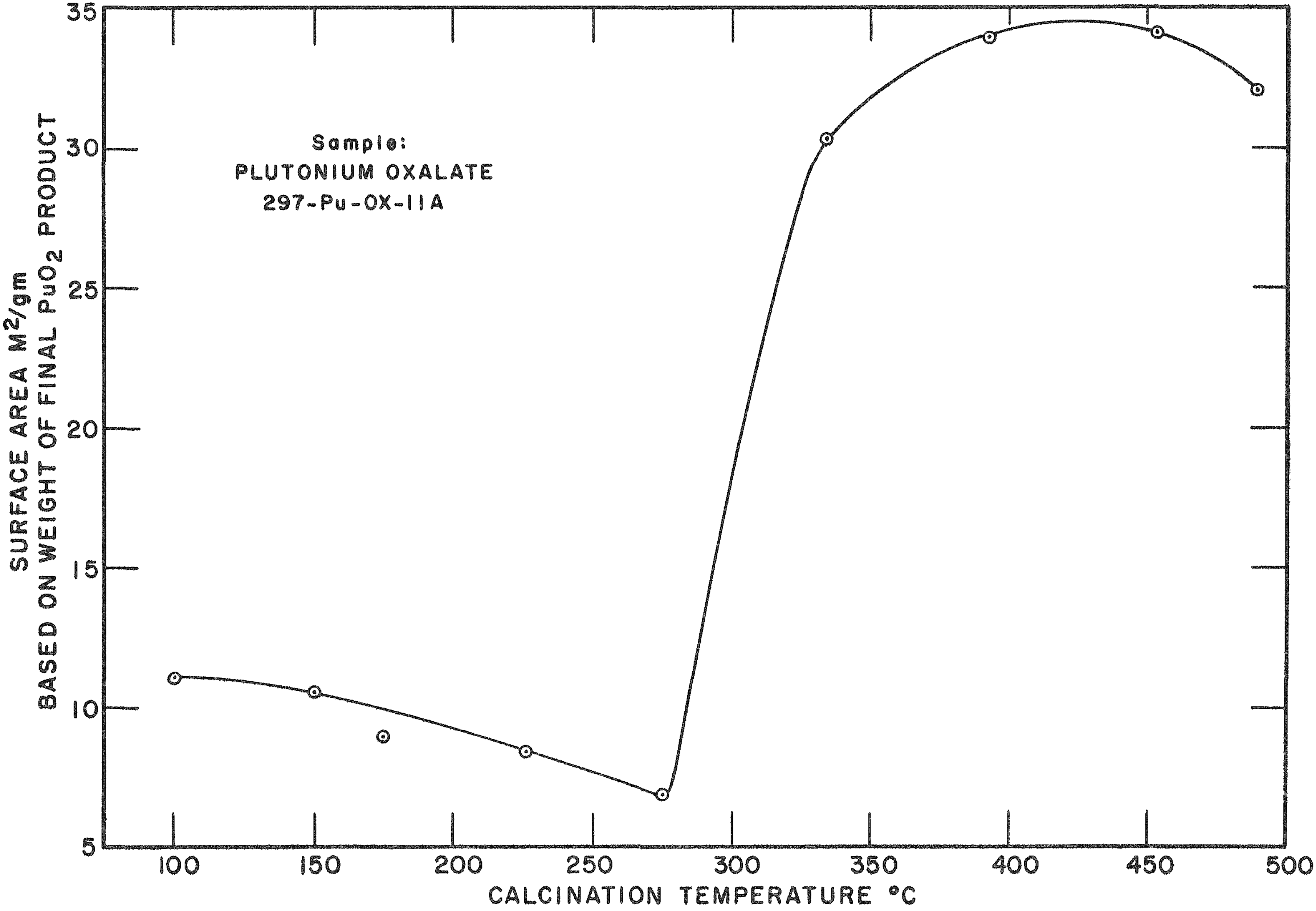

Figure-2.15

SURFACE AREA OF PLUTONIUM OXALATE DECOMPOSED IN SITU IN B.E.T. APPARATUS

The sudden rise in surface area at about 275°C is attributed to a breakdown in the crystallite structure caused by the many fissures that occur during crystal structure changes and during escape of decomposition gases. However, preliminary air-permeability average particle size measurements suggest that degradation of primary particles and agglomerates may also occur during calcination. These data are summarized in Table 2.3. If such a degradation in particle size occurs, it is expected that the heating rate employed during calcination (or the atmosphere employed as it affects the decomposition rate) would contribute to the final PuO_2 particle characteristics. Investigations of the precursor oxalate particle size are being continued in order to further illucidate on the physical decomposition mechanism. Such data will provide a basis for determining proper process control and quality control methods.

Preparation and Characterization of Mixed Plutonium-Uranium Oxides

(A. Biancheria, G. Ehrlich, E. E. Garcia, J. Goodman
R. A. Jaroszeski, H. Krake, P. Rey)

During this period, a number of essentially, production runs were carried out on these UO_2-PuO_2 mixtures in order to determine the degree of reproducibility. The developed data will make subsequent irradiation tests much more meaningful and if later desirable, reproducible.

Two lots of UO_2-5 w/o PuO_2 and nine lots of UO_2-0.5 w/o PuO_2 powder were prepared by continuous co-precipitation of ammonium diuranate-plutonium hydroxide from uranium-plutonium nitrate solution followed by the standard operations of filtration washing drying reduction, and hammer-milling. In addition, two lots of UO_2-20 w/o PuO_2 were similarly prepared with the only variable between these lots being the use of dilute or concentrated ammonia as the precipitant since earlier studies had indicated that this variable exerted an influence on the heat sensitivity of the product during reduction. The purpose of these runs was to prepare material for pellet fabrication by cold pressing and sintering and to determine process reproducibility in multiple runs, particularly in regard to final powder surface area, particle size distribution, and other physical characteristics. The total yield of oxide prepared was 7 800 gm with each lot comprising 600 gm.

The U-Pu nitrate feed solutions were prepared by mixing appropriate amounts of the constituent stock solutions and diluting to the desired concentration. The compositions were controlled within nominal limits of 0.5 ± 0.1, 5 ± 0.5, and 20 ± 0.2 w/o PuO_2.

For the two low Pu concentrations, separate streams of U-Pu feed solution and concentrated NH_4OH were introduced into a 4-liter precipitator containing a stirred 1700 ml water "heel". For the 20% concentration, no

Table 2.3

Air Permeability Average Particle Size
(microns)

Sample Identification	Calcination Temperature °C	$Pu(C_2O_4)_2$	PuO_2
297-Pu-9-Lot II	760	11.6	2.6
297-Pu-9-Lot III	350	14.6	1.6
297-Pu-9-Lot IV	760	8.3	3.6
297-Pu-11A	760	10.6	2.3

heel was used. The composition in the reactor thus changed continuously and approached steady state during each run. NH_4OH was added in calculated excess so that the liquor in the precipitating chamber was slightly basic. Under these conditions the formation of ADU and $Pu(OH)_4$ was almost instantaneous. The resulting slurry was moderately viscous and was easily agitated by the turbine-type stirrer. The temperature of the slurry was maintained at 55°C by circulating heated water through a 3 ft spiral of $\frac{1}{4}$ in O.D. stainless steel tubing immersed in the slurry. Slurry volume was maintained constant by periodically withdrawing slurry from the chamber and drawing it into a porous stainless steel filter cannister. In all cases, the solids separation was very good; in relatively few cases a small amount of solids was drawn through the cannister walls, but this was of short duration and caused negligible loss. The waste liquor was collected in tanks prior to disposal. At the completion of the run, the filter cannisters were flushed with water, aspirated for a few minutes and air-dried at 200°C overnight.

A complete summary of processing conditions for each of the eleven runs is given in Table 2.4. Average residence time was calculated from the feed rates in the precipitator.

The filtrate was checked periodically during each run and was found to have an average pH of 9 ± 0.5. Under these conditions, the precipitation is essentially complete. The waste liquor was checked for Pu content by a γ- counting procedure and was found to contain 5-20 mg Pu/l for all runs.

After overnight air drying, the contents of the filter cannisters were weighed and transferred to an inconel furnace flask. The oven-dried material was reduced in an atmosphere of N_2-6% H_2. The reduction cycle involved bringing the furnace temperature from ambient to about 740°C in one hour, holding at about 740°C for one hour and fifty minutes, cooling from about 740°C to ambient in one hour, and finally allowing the material to cool in the reducing gas atmosphere at room temperature for 20 hours.

After reduction, the UO_2-PuO_2 granules were converted to a uniform powder by hammer-milling. Each batch of material was separately milled. Less than 1% weight loss was experienced on hammer-milling these materials, including cleanup.

Samples of each lot were submitted for various physical and chemical tests including composition assay, trace analysis, oxygen/uranium ratio, surface area and particle size. The results of the chemical analyses are given in Table 2.5. The results of the various physical measurements are given in Table 2.6.

Average physical property measurements and percentage deviations calculated from the nine replicate data sets (Lots B1A through B2D) lead to the following conclusions:

Table 2.4

Summary of Conversion Processing Data Coprecipitated UO_2-PuO_2 Materials

Sample Identification	871-A1	871-A2	871-B1A thru B1E	871-B2A thru B2D	297-Pu-10	297-Pu-13
Precipitation Conditions						
Method	Continuous	Continuous	Continuous	Continuous	Continuous	Continuous
Temperature, °C	55	55	55	55	45	55
Feed Composition						
gm Pu/liter	6.2	5.7	0.5	0.5	20	28.9
gm U/liter	116.0	99.0	100	100	80	112
H^+, molarity	1.17	1.0	1.0	1.0	1.0	1.0
Feed Flow Rate, liters/hr	1.2	1.2	1.2	1.2	0.73	1.2
Precipitant Composition						
NH_4OH, molarity	14.5	14.5	14.5	14.5	3.5	14.5
Precipitant Flow Rate, liters/hr	0.33	0.33	0.33	0.33	0.57	0.3
Precipitation Average Holdup, minutes	30	67	67	67	36	70
Total Number Throughputs	10.2	4.5	4.5	4.5	13	4.5
Drying Temperature, °C	200	200	200	200	180	200
Furnace Conversion Conditions						
Reduction Temperature, °C	740 ± 5	740 ± 5	740 ± 5	740 ± 5	740 to 860°C	755 ± 5
Reduction Time, minutes	110	110	110	110	70	80
Gas Atmosphere	N_2-6% H_2	N_2-6% H_2	N_2-6% H_2	N_2-6% H_2	N_2-6% H_2	N_2-6% H_2

Table 2.5

Summary of Analytical Data
Co-precipitated UO_2-PuO_2 Materials

Sample Designation	% UO_2	% PuO_2	Spectrographic Trace Analysis														
			Fe	B	Cd	Mn	W	Al	Mg	Sn	Cu	Pb	Cr	Si	Ni	Mo	V
871-B1A	99.4	0.57	150	<0.2	<1	25	<1	<20	<20	<1	1	<5	<10	75	5	1	1
871-B1B	99.5	0.54	100	"	"	20	"	"	"	"	"	"	"	"	5	"	"
871-B1C	99.5	0.52	150	"	"	25	"	"	"	"	"	"	"	"	5	"	"
871-B1D	99.5	0.49	150	"	"	15	"	"	"	"	"	"	"	"	5	"	"
871-B1E	99.5	0.49	150	"	"	10	"	"	"	"	"	"	"	"	75	"	"
871-B2A	99.5	0.46	150	"	"	10	"	"	"	"	"	"	"	"	5	"	"
871-B2B	99.4	0.55	100	"	"	10	"	"	"	"	"	"	"	"	5	"	"
871-B2C	99.5	0.48	100	"	"	10	"	"	"	"	"	"	"	"	5	"	"
871-B2D	99.5	0.49	100	"	"	15	"	"	"	"	6	"	"	"	5	"	"

Table 2.6

Summary of Physical Powder Characteristics
Co-precipitated UO_2-PuO_2 Materials

Sample Designation	% UO_2	% PuO_2	Bulk Density gm/cc	Tap Density gm/cc	Air-Permeability Avg. Diameter microns	B.E.T. Surface Area M^2/gm	50% M.S.A. Particle Size** microns	Screen Analysis w/o Greater than 74 microns
871-A1	95.24	4.76	0.74	1.86	0.40	5.1	0.8	< 2
871-A2	95.45	4.55	1.20*	1.85	.40	7.08	0.50	< 2
871-B1A	99.4	0.57	0.70	2.08	0.40	5.5	0.8	< 2
871-B1B	99.5	0.54	0.71	2.09	0.39	4.7	0.5	< 2
871-B1C	99.5	0.52	1.42*	2.23	0.39	4.7	0.7	6
871-B1D	99.5	0.49	0.60	2.09	0.39	5.2	0.6	25
871-B1E	99.5	0.49	0.72	2.18	0.30	4.2	0.5	8
871-B2A	99.5	0.46	0.59	1.83	0.35	5.3	0.8	12
871-B2B	99.4	0.55	0.58	2.08	.53	5.5	1.0	26
871-B2C	99.5	0.48	0.67	2.12	0.44	4.8	0.7	12
871-B2D	99.5	0.49	0.73	1.99	0.43	5.2	0.95	6
Average			0.78±0.11	2.04±0.14	0.40±0.02	5.2±0.7	0.71±0.18	
297-Pu-10(a)		20	1.82	2.2	4.6	12.8		
297-Pu-10(b)		20				12.2		
297-Pu-10(c)		20				12.4		
297-Pu-10(d)		20				8.2		
297-Pu-13***		20	1.29		0.42	7.25	0.71	

* Verified by repeat measurement.
** Excluding particles of diameter > 74 microns.
*** Hammermilled.

a) Tap density variations from lot to lot averaged only ±7% while bulk density variations were twice as high.

b) Air-permeability particle size varied ±5% from the average.

c) Surface area variations averaged ±14% from lot to lot. (Approximately half this variation may be attributed to experimental error.)

The moderately low lot-to-lot property variations observed here indicate that adequate control of process conditions involving particle agglomerate characteristics (wet operations) and total surface area (furnace treatment) can be maintained during small-lot process development trials.

Examination of the tabulated data for the UO_2-20 w/o PuO_2 materials shows clearly that Lot 297-Pu-10, prepared with dilute ammonia, is distinctively different from Lot 297-Pu-13, prepared with concentrated ammonia. These data provide further evidence of the effects of reactant concentration on product surface area, as first seen comparatively between Lot 297-Pu-6 and -7(i). Reproducibility of product properties as prepared from concentrated ammonia appears to be good as can be seen by comparing the surface area of Sample 297-Pu-13 (7.25 M^2/gm) with the earlier Sample 297-Pu-6 prepared under the same conditions (7.1 M^2gm reported earlier(i)). Further data on 297-Pu-6 material shows the influence of reduction temperature on surface area. These data are presented in Figure 2.16; also shown thereon are similar data for dilute ammonia preparations. In contrast, it is to be noted that a temperature in excess of 850°C is required to initiate loss of surface area in mixed oxide material prepared with dilute ammonia.

By incorporation of the data developed during this period with pertinent results developed previously using the dilute ammonia process, one can ascertain the influence of oxide composition on the surface area. This variation is shown in Figure 2.17. Addition of plutonium results in an almost linear increase in surface area. In this effect, the property influence of ammonia concentration is reversed, and one finds that mixed oxides prepared by co-precipitation with concentrated ammonia have a final surface area (range 6-8 M^2/gm) which is relatively insensitive to plutonium concentration, due primarily to a leveling-out effect (i.e., reduction in surface area) which occurs during exposure to the 740°C environment during reduction. The final surface area can, of course, be controlled by the correct choice of furnace temperature in this case.

(i) NUMEC P-80, Progress Report, "Development of Plutonium-Bearing Fuel Materials", page 21.

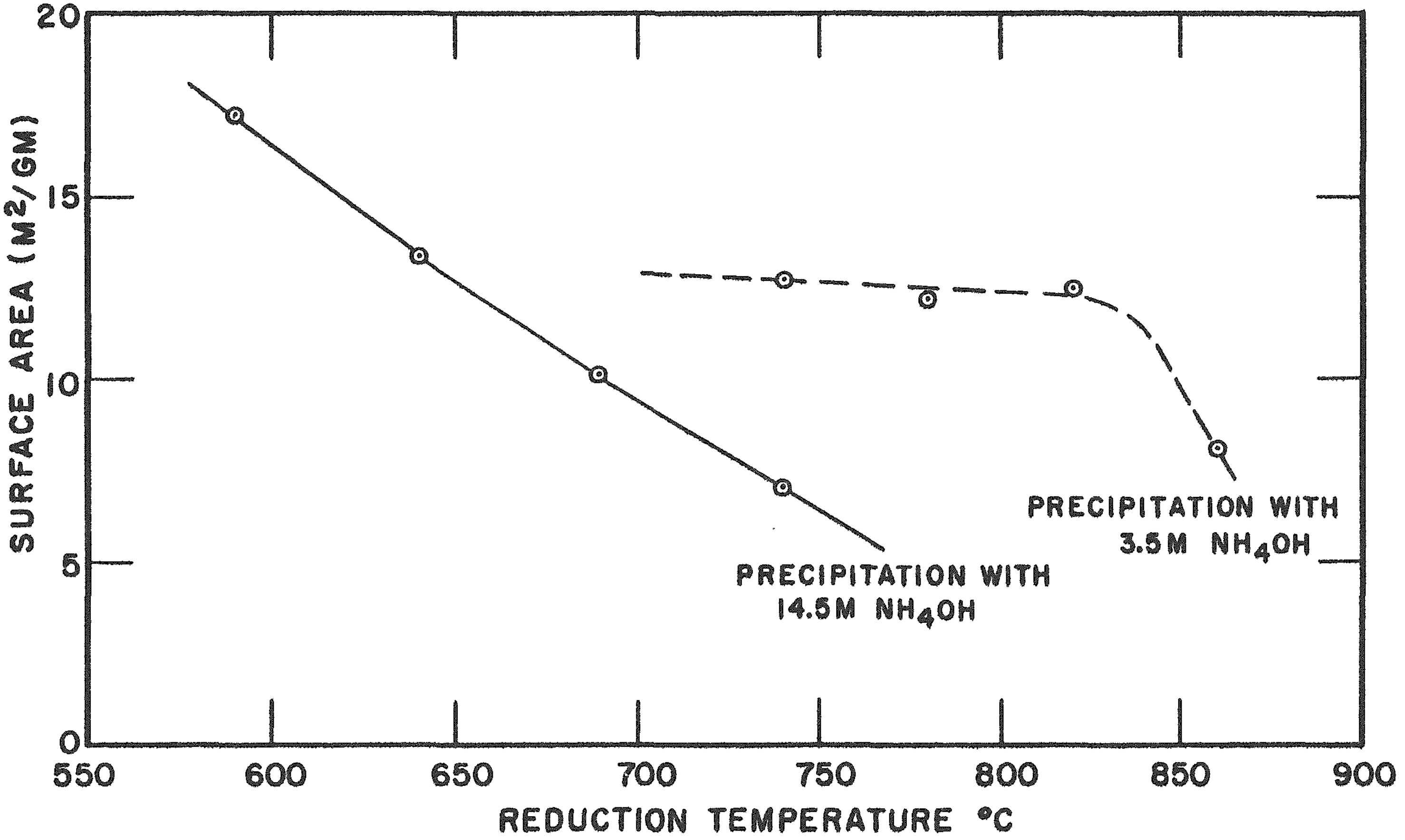

Figure - 2.16

EFFECT OF REDUCTION TEMPERATURE AND AMMONIA CONCENTRATION ON SURFACE AREA OF MIXED URANIUM - 20% PLUTONIUM OXIDE (CONTINUOUS PRECIPITATION PROCESS, -70 MINUTE REDUCTION)

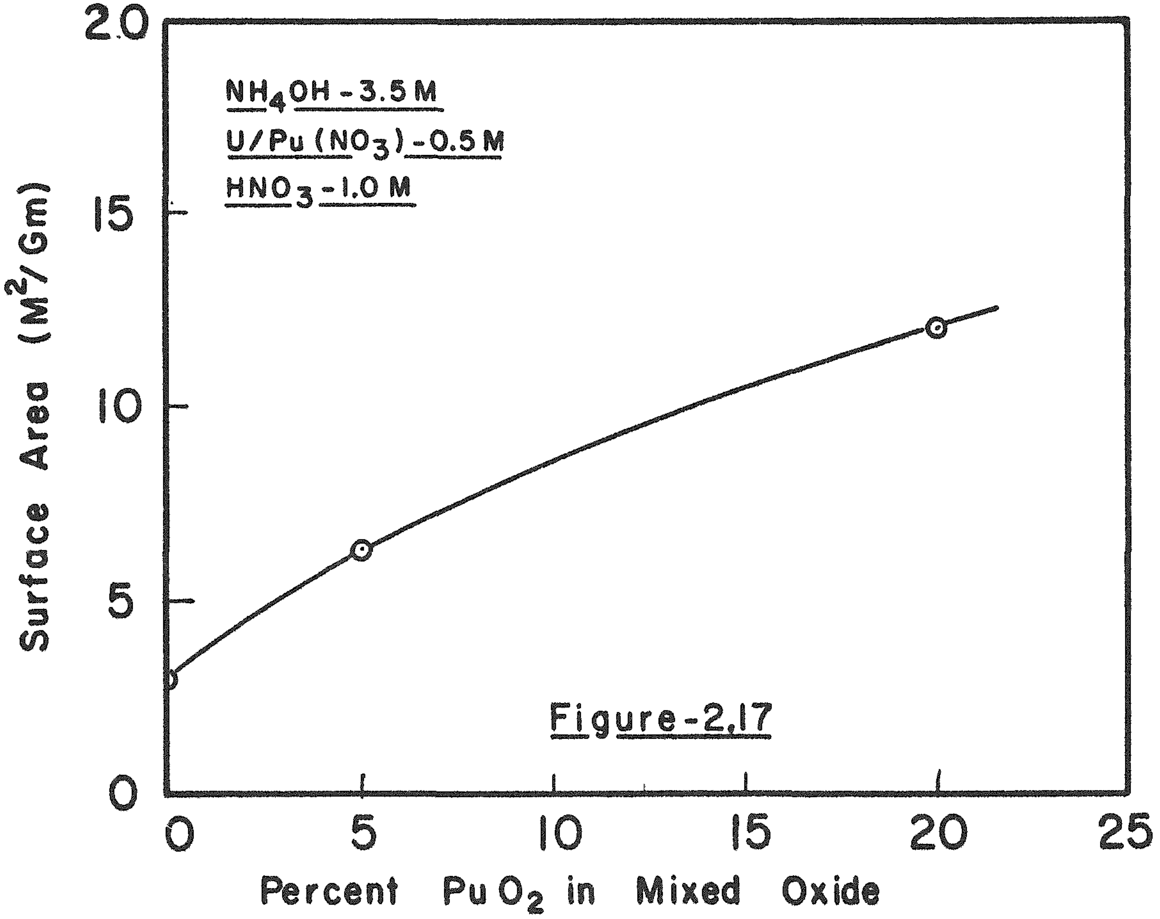

Figure-2.17

EFFECT OF COMPOSITION ON SURFACE AREA OF URANIUM / PLUTONIUM DIOXIDE

CONTINUOUS PRECIPITATION PROCESS - 70 MINUTE REDUCTION AT 740 °C

Preparation and Characterization of High Density Granular Oxide Powders

(G. Ehrlich, A. Biancheria, J. Goodman, J. Miles)

As part of a program for the direct preparation of dense, coarse UO_2-PuO_2 and PuO_2 powders for use as mechanical packing, swaging or plasma torch feed, several prototype preparations of UO_2 have been examined. The data and methods developed from these lab scale experiments will be applied to the glove box preparation of powders containing PuO_2. The preparation routes examined include homogeneous precipitation employing uranyl nitrate hexahydrate (UNH) and urea uranyl sulfate and urea, and UNH and ammonium carbonate. The direct precipitation of uranium(IV)oxalate was also examined. Processing conditions for four UNH-urea runs were presented earlier(1); similar data for samples prepared during this reporting period are presented in Table 2.7. Precurser powder characteristics produced under these conditions are presented in Table 2.8.

The effect of preparation conditions particularly reactant concentrations and drying temperature, upon the properties of the intermediate ADU is seen to be significant for material precipitated by the hydrolysis of urea. Comparison of characterization data from ADU samples, 1405, 1406, 1411, 1412, 1413 and 1414 shows that remarkably high ADU tap densities resulted from use of high reactant concentrations. Drying at 95°C produced a higher ADU density than drying at 25°C. The low ADU surface areas (0.12 and 0.07 M^2/gm respectively) correspond to equivalent sphere diameters of 9 and 15 microns respectively, for samples 1414 and 1413. The close agreement between these derived particle diameters, the air-permeability average diameters and microscopically-measured diameters, correlates well with the high observed tap density of these materials. The UO_2 derived from sample 1413 by reduction for 1 hour at 740°C (shown in Figure 2.18) accordingly had high bulk density (3.2 gm/cc) together with high surface area. The effects of high-firing with regard to further densification will be studied shortly

Characterization data for the UO_2 samples prepared by these methods are summarized in Table 2.9. With the exception of sample 1415, a coarse particle size, as determined by the Mine Safety Appliance method, was obtained. The high surface areas, however, indicate that these UO_2 particles have a considerable degree of fine pore structure. Comparison of the surface areas of the precursor powders with the corresponding UO_2, Table 2.10 shows that this fine pore structure originates in the conversion step. A similar pheonmenon was observed in the conversion of plutonium oxalate and was discussed in a previous section of this report.

---

(1) NUMEC P-80 Progress Report, "Development of Plutonium-Bearing Fuel Materials" page 29.

Figure 2.18

Granular UO_2

(150X) Sample 1413

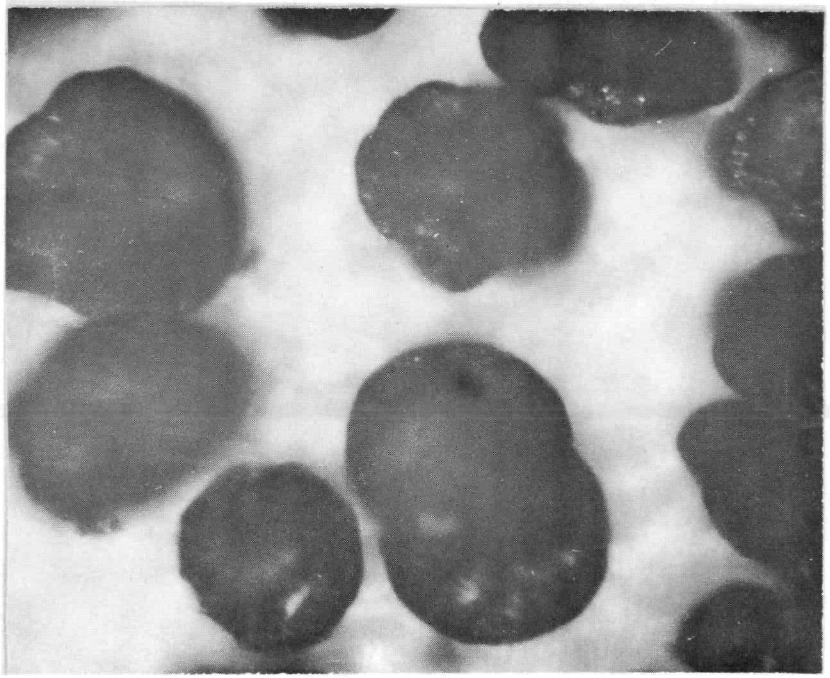

Figure 2.19

Granular UO_2

(350X) Sample 1420

Table 2.7

Process Conditions
Granular Oxide Preparation Routes

Experiment Number	19-4-8	19-9-2	19-15-36
Sample Number	1409	1415	1420
Uranium Starting Solution	UNH	UNH	UO_2SO_4
Uranium Concentration, M	0.5	0.5	0.5
Precipitant	$H_2C_2O_4$	$(NH_4)_2CO_3$	$(NH_2)_2CO$
Precipitant Concentration, M	7.5(50% XS)	2.0	7.5
Precipitant Addition Time, hrs	rapid	1	rapid
Reaction Temperature, °C	$\sim$100	$\sim$100	$\sim$100
Reaction Time, hours	1	1	16
pH of Mother Liquor			$\sim$7
Drying Temperature, °C	90	95	100
Drying Time, hours	2	16	2
Reduction Temperature, °C	740	740	740
Reduction Time, hours	1	1	1
Furnace Atmosphere	N_2-6% H_2	N_2-6% H_2	N_2-6% H_2
Batch Size, gm U	50	50	50

Table 2.8

Powder Characteristics of Precursor Granular Oxide Preparation Routes

Sample Number	Preparation Route	Drying Conditions		Bulk Density gm/cc	Tap Density gm/cc	Average** Particle Diameter microns	Surface Area M^2/gm
		Temp °C	Time hrs				
1405	UNH + $(NH_2)_2CO$*	25	24	1.25	1.37	7.8	1.17
1409	$UO_2(NO_3)_2 + H_2C_2O_4$	90	2	0.59	1.02		0.48
1411	UNH + $(NH_2)_2CO$*	25	24	1.32	1.67	7.3	0.67
1412	UNH + $(NH_2)_2CO$*	65	24	1.34	1.65	5.8	1.12
1413	UNH + $(NH_2)_2CO$*	25	24	1.95	2.16	15.2	0.07
1414	UNH + $(NH_2)_2CO$*	95	16	2.36	2.46	17.0	0.12
1415	UNH + $(NH_4)_2CO_3$	95	16				3.62
1420	$UO_2SO_4 + (NH_2)_2CO$	100	2	1.54	1.90	11.0	0.95

* Preparation described in NUMEC P-80, page 29.

** Air-permeability method.

Table 2.9

Characteristics of UO_2 Powders Granular Oxide Preparation Routes

Sample Number	Preparation Route	Conversion* Temperature °C	Bulk Density gm/cc	Tap Density gm/cc	Average** Particle Diameter microns	Surface Area M^2/gm	50%*** Particle Size microns	O/U Ratio	Physical Appearance
1405	UNH + Urea	540	-	1.84	3.6	9.6	37	-	Mixture of spherical and irregular granules.
1405	UNH + Urea	740	-	-	3.5	-	41	-	Mixture of spherical and irregular granules.
1406	UNH + Urea	540	-	2.02	5.1	6.0	50	2.16	Mixture of spherical and irregular granules.
1406	UNH + Urea	740	-	2.05	5.0	7.1	45	2.10	Mixture of spherical and irregular granules.
1409	$UO_2(NO_3)_2$ + Oxalic Acid	740	0.66	1.27	3.1	12.6	11	2.46	Needle-like crystals (length 15-60 μ)
1413	UNH + Urea	740	-	3.2	8.0	14.3	23	2.23	Smooth, nodular granules, $<50\mu$
1415	UNH + $(NH_4)_2CO_3$	740	0.86	1.40	0.73	4.5	1.0	2.18	Irregular rounded granules, fuzzy surface.
1420	UO_2SO_4 + Urea	740	1.74	2.03	6.3	4.8	2.2		Smooth rounded granules and spheres, $<120\mu$

* Two hours at temperature, 6% H_2-94% N_2

** Air-permeability method.

*** Sedimentation method, shaker dispersion.

Table 2.10

Comparison of Surface Areas of UO_2 with Precursor Powders

Sample Number	Precursor	Surface Area M^2/gm	
		Precursor	UO_2
1405	A.D.U.	1.2	9.6
1409	Uranium Oxalate	0.48	12.6
1413	A.D.U.	0.07	14.3
1415	A.D.U.	3.62	4.3
1420	A.D.U.	0.95	4.8

The physical appearance of the granular UO_2 products, taken together with physical data from Table 2.9 shows, for example, that sample 1413 is composed primarily of partially densified, strongly-bound agglomerates, while samples 1405 and 1406 are composed of larger, less densified agglomerates. Samples 1415 ADU and UO_2, precipitated by hydrolysis of ammonium carbonate, rather than urea, were composed of "snowball" agglomerates up to 250 microns in. dia., which appear weakly bonded together, as evidenced by the 1.0 micron average sedimentation particle size and 0.7 micron average air permeability particle size. Sample 1420 (shown in Figure 2.19) contained previously strongly-bound, large agglomerates. Sample 1409, representing a different class of material, consisted of separate needle like crystals, whose average dimensions, as determined by microscopy, corresponded with the air-permeability average diameter.

A glove box is presently being equipped to allow extension of this effort to PuO_2-UO_2 and PuO_2.

Analytical Chemistry

(O. Menis, W. Judd, E. E. Garcia
P. Rey, R. A. Jaroszeski)

The analytical studies during the past quarter included the development of procedures for potentiometric titration of plutonium, the initiation of studies of the polarographic determination of oxygen to metal ratio in plutonium-uranium oxide mixtures, the adaptation of x-ray fluorescence and gamma counting to low level plutonium residue analysis and the α ray spectrometry of plutonium and other transuranium elements.

Potentiometric Titration of Plutonium

A new approach to the potentiometric titration of plutonium has been developed; this involves the oxidation of plutonium to the hexavalent state, then reduction to the quadrivalent state with excess ferrous ion and the back titration of the excess with a standard dichromate solution. The established methods of potentiometric titration involve only one electron change in the titration Pu (III) to Pu (IV). In the above described modification, the sensitivity of the method is thus doubled. The steps in the procedure involve first oxidation of plutonium with argentic peroxide in a 1N sulfuric acid solution. The excess oxidizing agent is then decomposed by heating. Then an excess of previously standardized ferrous solution is added and back titrated with standard 0.500 N potassium dichromate. The titration is carried out in a volume of 10 milliliters with platinum calomel electrodes. At the end point when titrating 1 to 5 milligrams of plutonium the potential break is approximately 50 millivolts. On test solutions, the agreement between this method and the amperometric method(1)

---

(1) NUMEC P-70, Progress Report, "Development of Plutonium-Bearing Fuel Materials", page 21.

was within 0.3 per cent. The new procedure can be carried out more rapidly than the former and eliminates the necessity of using an agar bridge to the reference cell. This bridge has been found to be a source of trouble because it is difficult to keep decontaminated and stable and therefore requires frequent replacement.

Oxygen/Metal Ratio in Mixed Oxides

In the evaluation of preparations of mixed oxides, the ratio of oxygen to metal is of importance. In the case of uranium dioxide alone, two methods have been used most extensively; one involves the conversion of the dioxide to U_3O_8, and the other involves the polarographic determination of uranium (VI)(i). Because of the possible presence of lower oxides of plutonium, the latter method appears to be more suitable to the evaluation of the stoichiometric composition of mixed oxides. Also, the simultaneous determination of several species and oxidation states in the original mixture is possible. A study was, therefore started to ascertain the best conditions for dissolving the mixed oxides without altering the original oxidation states or causing interaction between the components. Work was also initiated to determine the sensitivity and accuracy of the polarographic method for the determination of uranium (VI) by means of an ORNL Model Q-1988 controlled potential and derivative polarograph(ii)(iii).

Standards and Reagents: Standards and reagents were prepared as follows:

Standard Uranium (VI) Solution - This solution was prepared from high purity uranium dioxide dissolved in nitric acid and converted to the sulfate by fuming with sulfuric acid. The final uranium concentration was determined by the Jones reductor-dichromate titration method.

Standard Uranium (IV) Solution - This solution was prepared by the reduction of uranium (VI) sulfate solution in a Jones reductor and aeration to eliminate traces of uranium (III). To this solution 40 ml of concentrated phosphoric acid and 50 ml of 0.2N perchloric acid were added and the volume adjusted to 100 ml with doubly deionized water.

Phosphoric Acid: Phosphoric acid of Analytical Reagent grade showed a very high background when used directly (see Figure 2.20). An effective purification was achieved by adding a potassium permanganate solution to the

---

(i) Kubota, H., Anal. Chem. 32 610 (1960)

(ii) Kelley, M. T., Jones, H. C., and Fisher, D. J., Anal. Chem. 31, 1475 (1959)

(iii) Kelley, M. T., Jones, H. C., and Fisher, D. J., Anal. Chem. 32 1262 (1960)

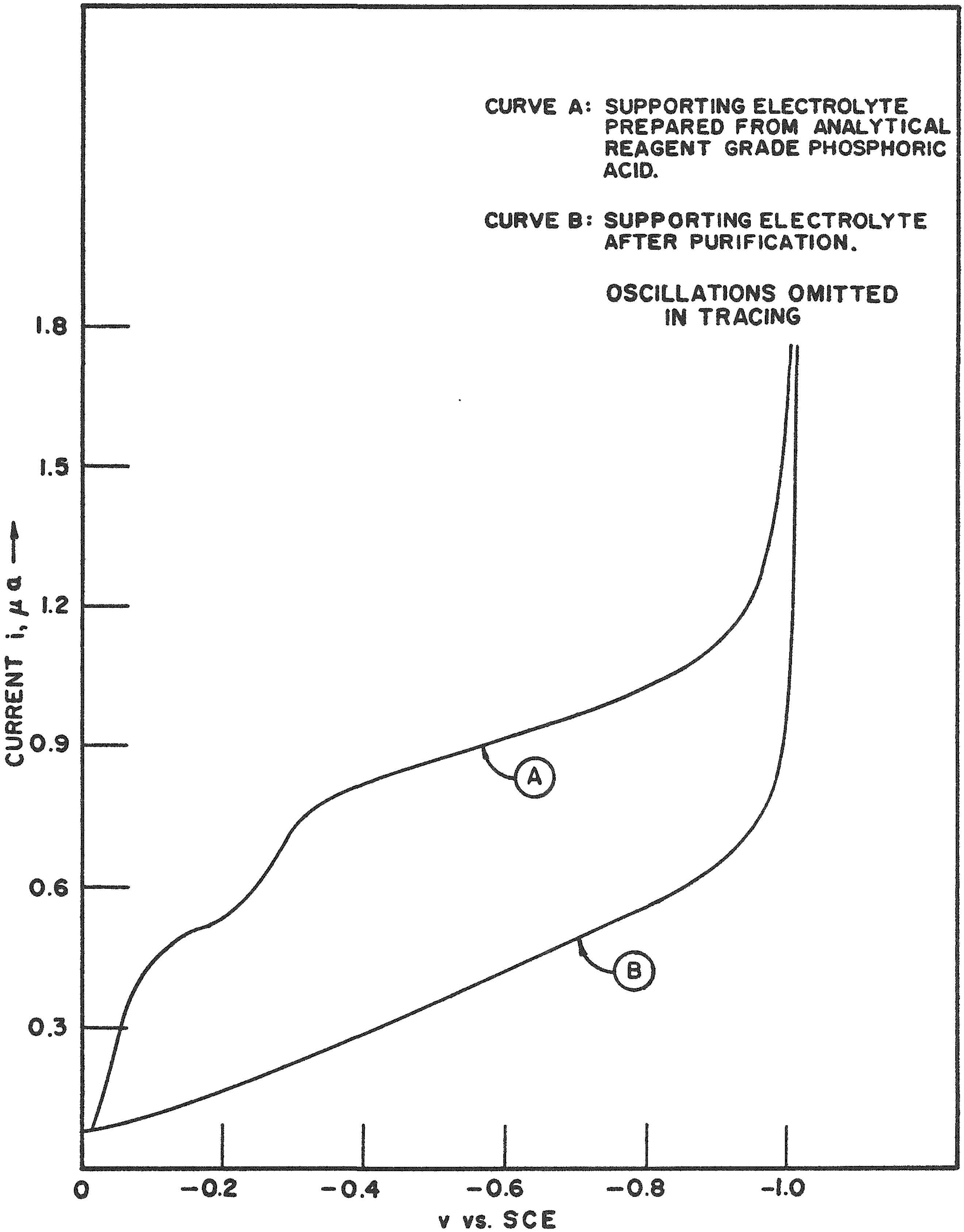

Figure 2.20

POLAROGRAM OF THE BACKGROUND CURRENT

hot acid until a permanent pink color was obtained and then reducing the excess with a small amount of sodium sulfite. The excess sulfite was eliminated by bubbling helium through the acid for one hour. After this procedure, the background was reduced as shown in Figure 2.20, curve B.

Experimental: The polarographic determinations were carried out in a cell made out of a 50 ml beaker covered with a rubber stopper with holes for admission of a dropping mercury electrode, a saturated calomel electrode (Beckmann #39270), a platinum anode and a glass tube for bubbling helium through the solution.

Polarograms were obtained between +0.15 and -0.60 v vs SCE, and in all cases, the standard addition technique was used. The solution was deaereated after each addition, and a blanket of inert gas was kept over the solution during the determinations.

Results: Polarograms of uranium (VI) at two concentration levels and using two techniques, one a peak follower, the other the derivative polarogram, are present in Figures 2.21, 2.22, 2.23, and 2.24. These tests were carried out in the presence and absence of uranium (IV) and with several acid mixtures. The acid media tested were phosphoric, phosphoric-perchloric, phosphoric-sulfuric and mixtures. In all cases, a well-defined polarographic wave was obtained with half wave potential of 0.084 v vs SCE in the first medium and 0.03 v vs SCE in the mixed acids. With the ORNL Model Q-1988 Polarograph it is possible to produce different types of polarograms. Two of these, peak follower and derivative type, were studied because of their special characteristics. As shown in Figure 2.21, the peak follower setting yields an undampened polarogram of the maxima of oscillations and thus is free of errors due to excessive damping. The derivative circuit offers polarograms shown in Figure 2.22 and 2.23 which are easier to measure and have higher sensitivity. The respective sensitivities were 0.013 and 0.06 microampere per microgram of uranium, or approximately a four-fold enhancement for the derivative method. At two levels of uranium (VI) concentration, 40 to 120 microgram and 4 to 12 micrograms, a linear relationship was obtained (Figures 2.21a and 2.22a). With the lower concentrations, however, the precision was poorer and a bias was noted. This is in part due to the proportionally greater effect of small amounts of impurities present in the supporting electrolyte. From a comparison of the derivative polarograms and the peak follower at very low concentrations of uranium (VI), presented in Figures 2.23 and 2.24, it is also evident that the former is easier to measure even in the presence of a relatively large background current. Future studies will take into account the other parameters involved in the measurement of uranium (VI) in mixed oxides.

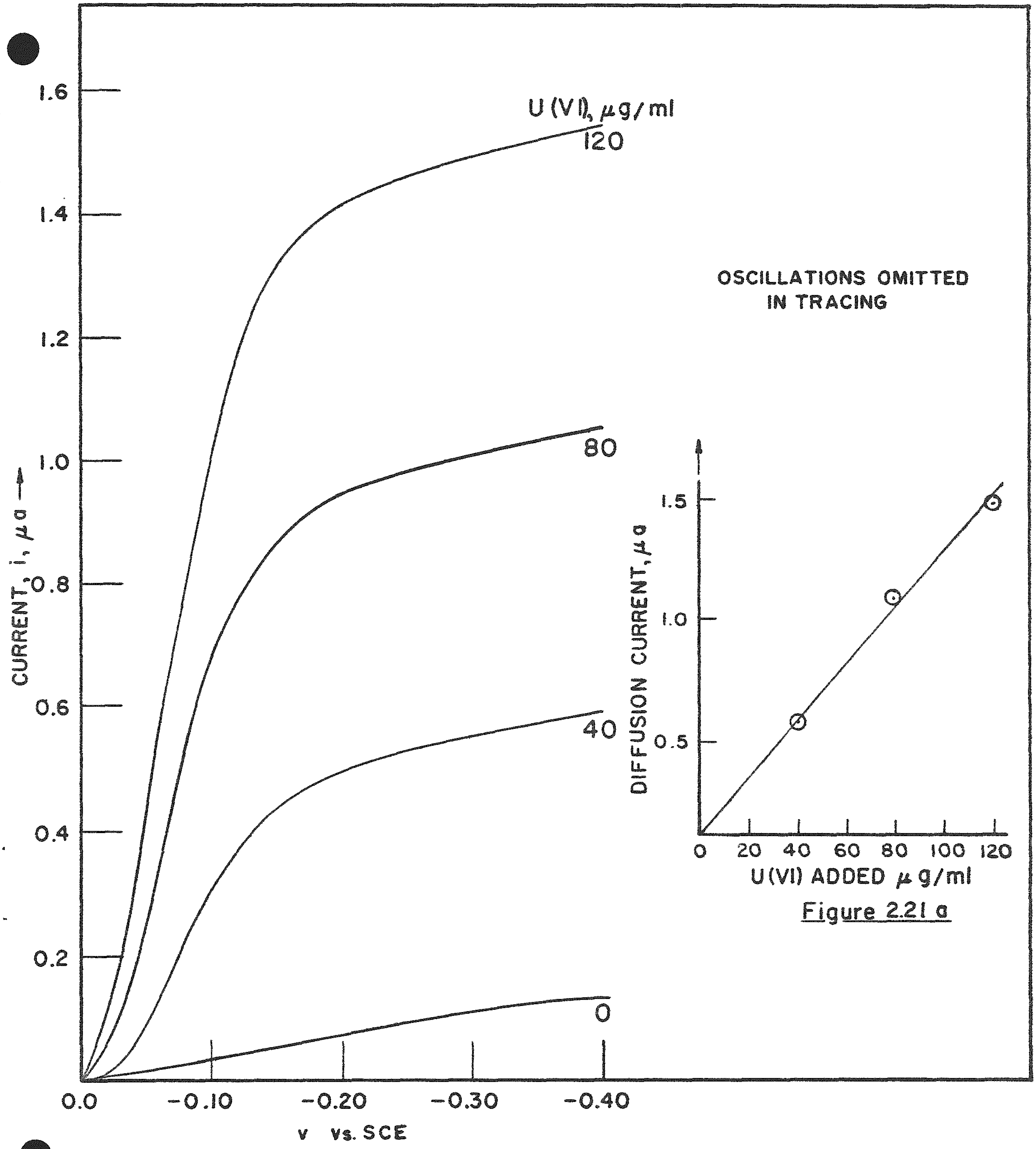

Figure 2.21 a

Figure 2.21

POLAROGRAPHY OF U(VI) IN 36% PHOSPHORIC-0.1 N PERCHLORIC ACID (PEAK FOLLOWER SETTING)

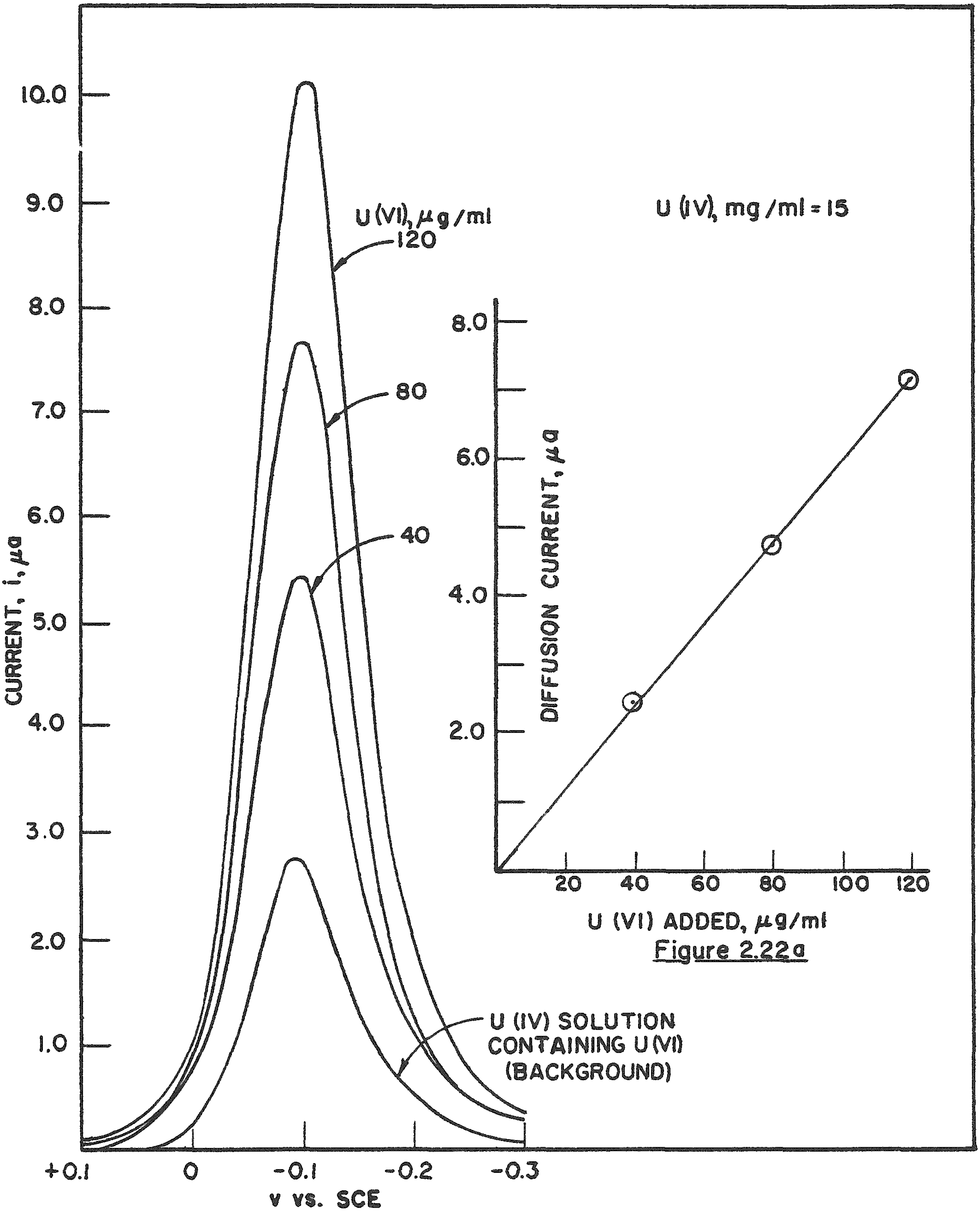

Figure 2.22a

Figure 2.22

DERIVATIVE POLAROGRAPHY OF U (VI) IN PRESENCE OF U (IV) IN 36 % PHOSPHORIC - 0.1 N PERCHLORIC ACID

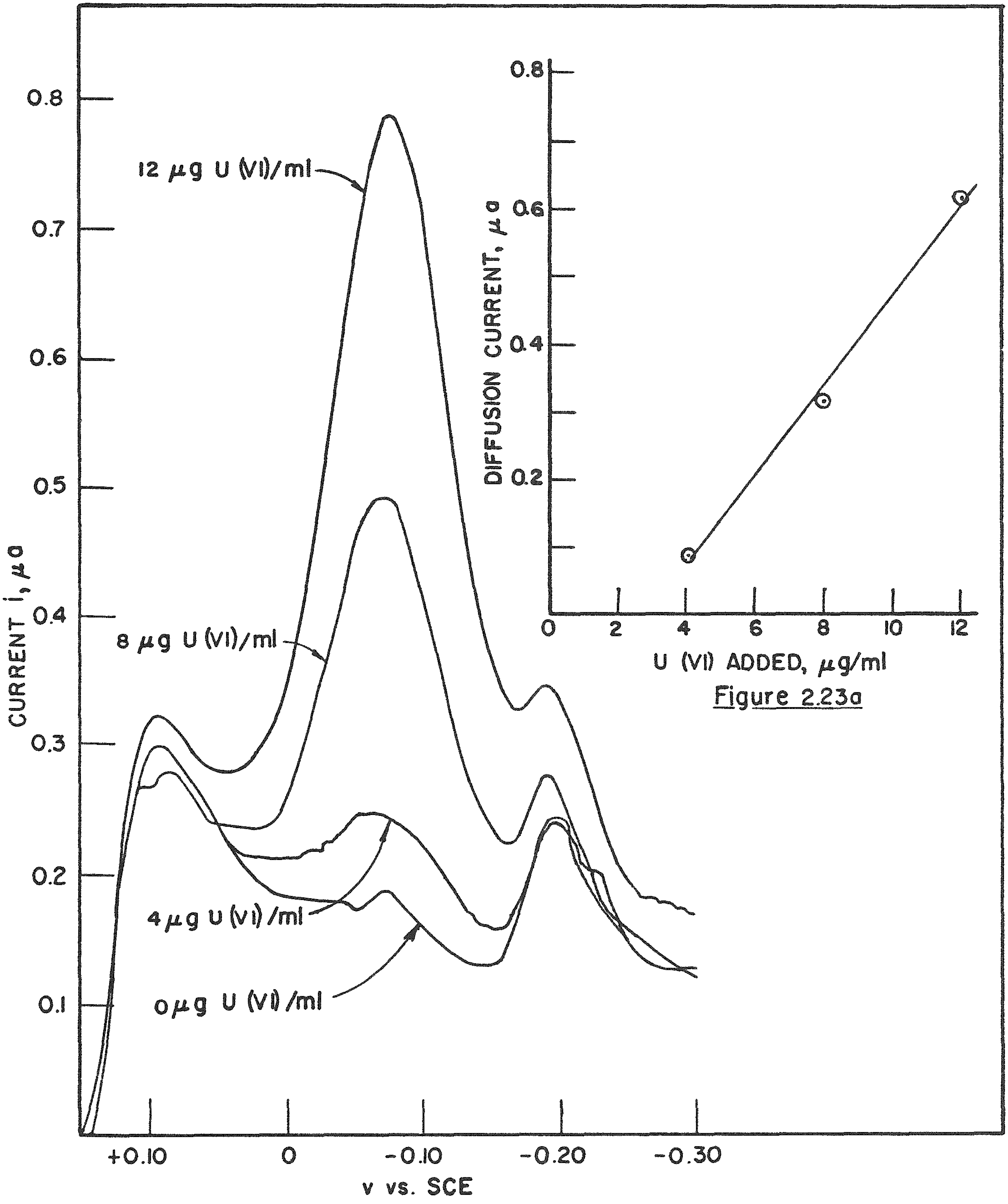

Figure 2.23

SENSITIVITY OF THE DERIVATIVE POLAROGRAPH FOR MICROGRAM AMOUNTS OF U (VI) IN 36 % PHOSPHORIC-0.1 N PERCHLORIC ACID

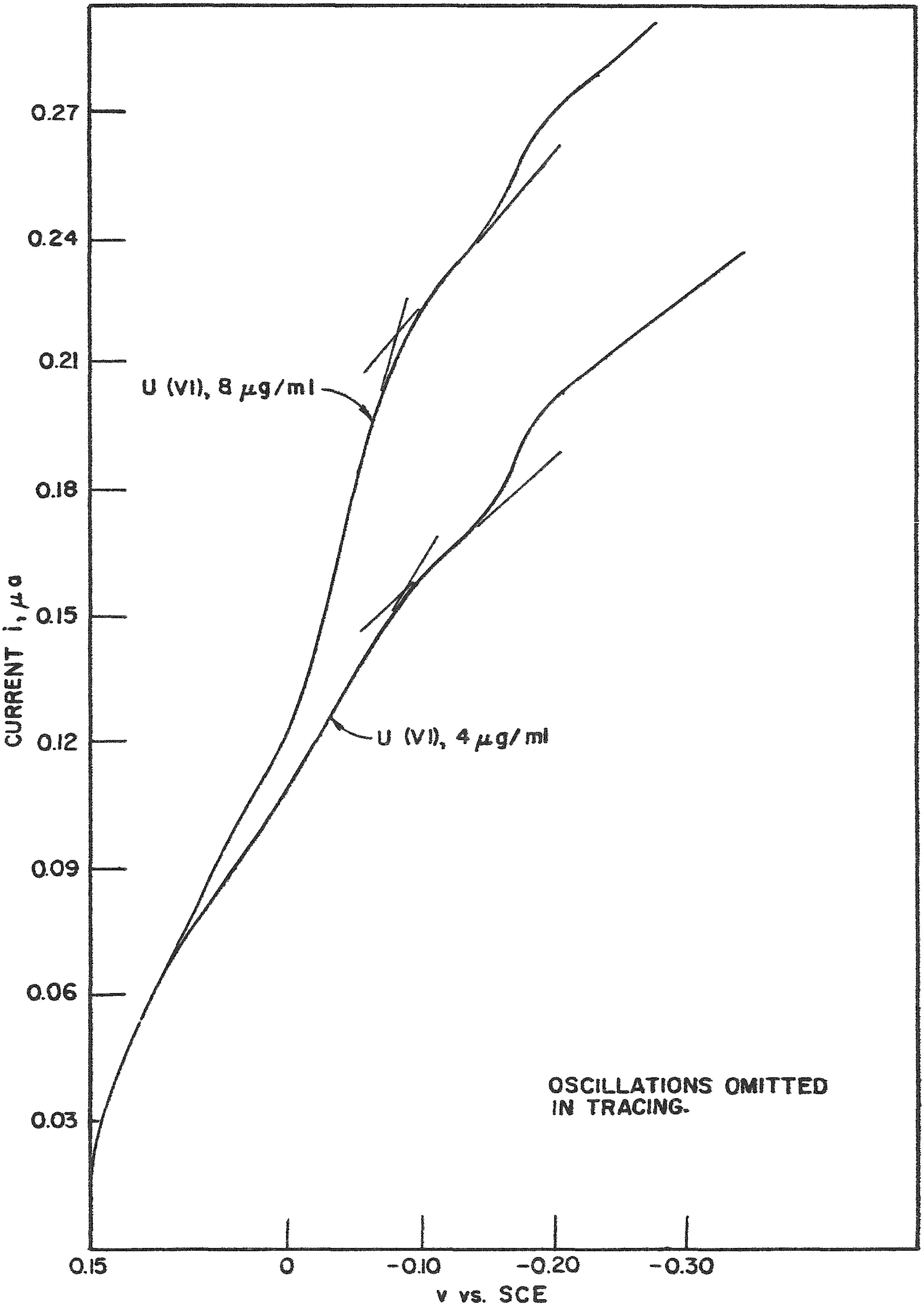

Figure 2.24

POLAROGRAPHY OF μg AMOUNTS OF U (VI) USING "PEAK FOLLOWER" POLAROGRAM IN 36% PHOSPHORIC-0.1 N PERCHLORIC

X-Ray Fluorescence Analyses

X-ray fluorescence techniques are being examined to evaluate their usefulness in analyzing for plutonium in the presence of uranium. Such a method has been described by Turnley(i). In our glove box setup, resolution is adequate to separate the strongest lines, as shown in Table 2.11. A study is now being made to determine the minimum detectable quantities of plutonium and uranium in order to evaluate the use of x-ray fluorescense techniques for the rapid examination of waste solutions.

γ-Counting

The study of gamma counting as a means for estimating the concentration of plutonium in waste solutions has been continued. The gamma ray spectra, shown in a previous progress report(ii), were found to be of sufficient intensity to enable one to estimate the plutonium concentration in dulute solutions. For this purpose a calibration curve was developed with solutions which were previously standardized by amperometric titration. Unknown waste solutions contained in similar containers were then counted and their concentration ascertained.

In this connection, a number of corrections should be made to the table presented in the previous progress report(ii). The 146 kev peak should be assigned to Pu-241 instead of to Pu-240; the 17 kev x-ray should have been designated as L series, and the 100 kev x-ray as K series.

Alpha Spectrometry

Alpha spectrometry as a convenient means for the determination of α-emitting components present in a plutonium solution was studied with the aid of crystal detectors. For this purpose, a silicon diode detector was used in conjunction with a Development Products Amplifier, Model SS-2000, and a Nuclear Data, Model ND-101, 256 channel analyzer. For recording the data,

---

(i) Turnley, W. S., "X-Ray Fluorescence Analyses of Plutonium", Third Conference on Analytical Chemistry in Nuclear Reactor Technology, Gatlinburg, Tennessee, 1959.

(ii) NUMEC P-70, Progress Report, "Development of Plutonium-Bearing Fuel Materials", page 36.

Table 2.11

Relative Intensities and Resolution of U and Pu Principle X-ray Fluorescence Spectra

Line	Scattering Angle, °		Relative Intensity
	Uranium	Plutonium	
L_{α_1}	26.13	24.91	100
L_{β_1}	20.59	19.39	80
L_{β_2}	21.60	20.57	60
L_{γ_1}	17.56	16.54	40

a Mosley X-Y recorder was utilized. Spectra of standards and samples were obtained from sources prepared by an electrolytic technique described by Ko(i)(ii). These sources, prepared on mirror polished platinum, were less than 0.001 micron thick, thereby eliminating most of the effects due to self-absorption. Standard solutions of Pu-239 and Am-241 were prepared after an anion resin separation and these were used to calibrate the instrument. Finally, a solution containing a mixture of transuranium elements and their isotopes was analyzed. The data are presented in Figure 2.25 and Table 2.12. The peaks due to Pu-239 and Pu-240, shown in this Figure, coincide with those of the pure standards, within the 0.9% resolution value, at this energy level. The peak observed at 4.93 Mev is due to the presence of Pu-242. Any contribution to this peak from Pu-241 (4.882 Mev) can be ignored due to its relatively low abundance. The peak at 5.47 Mev is due to Am-241. Since the other isotopes of Americium differ in energy by 4%, these could be resolved, thereby it is concluded that these were not present. Some Cm-243 and Cm-244 was found as indicated by a peak at 5.77 Mev. Other higher isotopes, presumably, were not detected because of their relatively short half-lives. Based on these preliminary data, the relative ratio of Am and Cm to Pu was 0.03 and 2×10^{-5} per cent, respectively. It is planned to extend this method to the quantitative estimation of plutonium in various stock solutions.

(i) Ko, R., Nucleonics, 15, 1 72-77 (1957)
(ii) Ko, R., Nucleonics, 14, 74 (1956)

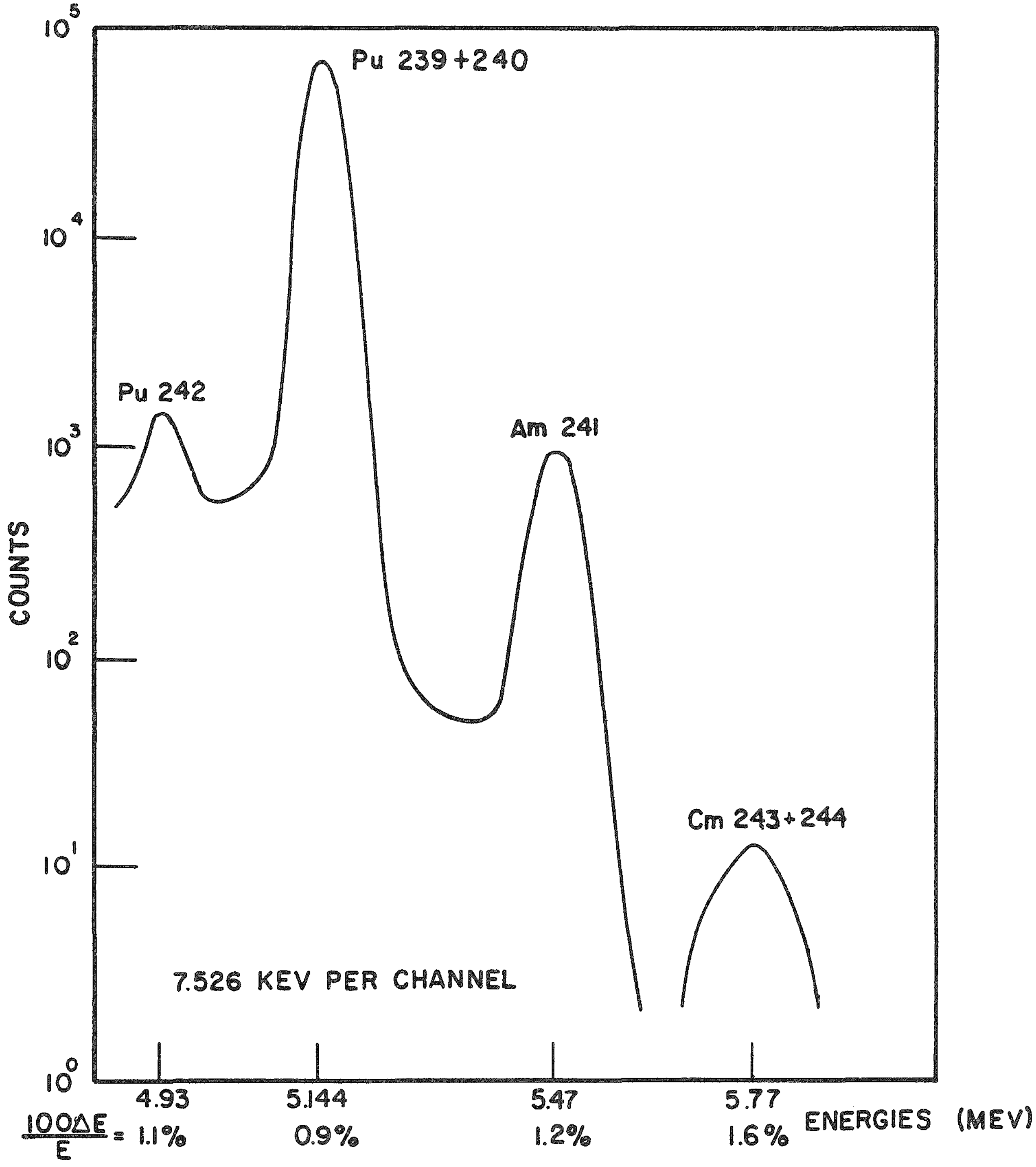

Figure 2.25

ALPHA SPECTRA OF Pu, Am AND Cm
A SOURCE, .001 μ THICK, ELECTRODEPOSITED
ON MIRROR-POLISHED PLATINUM

Table 2.12

Alpha Spectrometry of Transuranium Elements

Isotopes	Resolution $\frac{\Delta E}{E}$ x 100	Alpha Peaks (MEV) (i)(ii)	
		Found	Literature
Pu-241	1.1	4.93	4.887
Pu-239 Pu-240	0.9	5.14	5.144^x
Am-241	1.2	5.47	5.475^x
Cm-243 Cm-244	1.6	5.77	5.773 5.778

x standards

(i) Dzhelepov, B. S. and Peker, L. K., Decay Schemes of Radioactive Nuclides, Pergamon Press, 1961.

(ii) Sullivan, W. H., Trilinear Chart

FABRICATION AND EVALUATION OF FUEL SHAPES

Task 3.00

E. K. Halteman L. J. Jones

Mixed Oxide Sintering Studies

(R. M. Horgos, D. Houston, J. Miles)

Investigation of the fabrication of UO_2-5 w/o PuO_2 pellets by the cold press and sinter procedure was continued. The powder was co-precipitated as ammonium diuranate and plutonium hydroxide, and calcined in nitrogen-6% hydrogen at 750°C to yield the dioxides. As calcined and reduced, this powder lot (297-Pu-8) consisted of very hard, coarse aggregates unsuitable for pelletizing. The aggregates were broken up by hammer-milling through a "Mikro" pulverizer. Since the bulk density of the hammer-milled powder was low, slug pressing prior to cold compaction was found necessary. Slugging was done at 6 TSI and the slugged material reduced by impact fracture through a 40 mesh screen. The resultant material could be successfully compacted at 8-9 TSI without the aid of organic binders. Pellets that had been pressed at 12 TSI were overpressed, with resultant lower sintered densities and conical end cracking. All pellets were fired at 1600-1650°C for one hour in a nitrogen-6% hydrogen atmosphere with a four-hour heating cycle and a four-hour cooling cycle. Compaction and sintering characteristics are given in Table 3.1. The weight loss on firing is attributed to the burnoff of residual carbon from incomplete decomposition of the oxalate(i).

Two phenomena related to the firing process, one concerned with fracturing of the sintered pellets and the other with the appearance of a glassy coating on pellet surfaces, were observed. Approximately 15% of the sintered pellets which had been pressed at 8-9 TSI were found to have separated into two cylindrical pieces or into two conical ends with a cylindrical body. In both cases, a rather large impurity or inclusion was found at the parting interface. Further investigation by x-ray and spectrographic techniques is underway to determine the composition of the inclusions. A glassy substance was observed only on certain pellets and seemed to be related to the pellet position in the sintering boat. The pellets which were met by the purging gas (N_2-6% H_2) had clean surfaces while those that were downstream from the gas inlet had the glassy surfaces. The appearance of the glass is not related to any furnace position since the good pellets traverse the same regions as the bad ones. These two phenomena may be interrelated, but further investigation is necessary for clarification.

(i) NUMEC P-80, Progress Report, " Development of Plutonium-Bearing Fuel Materials", page 19.

Table 3.1

Compaction and Sintering Data
UO_2-5 w/o PuO_2
(Sintering at 1600°C for 1 hour)

Compaction Pressure TSI	Green Density, gm/cc	Fired Density, gm/cc	Firing Shrinkage, %	Weight Loss on Firing, %
8	4.87	10.39	22	1.22
9	4.93	10.44	22	1.23
12	5.19	10.08	*	1.22

* Conical end cracking.

To investigate the effects of reusing fired pellet material, fired pellets of UO_2-5 w/o PuO_2 were broken up in a steel die and further reduced in a tungsten carbide mill (Spex mill). This powder was added to the original hammermilled powder in the proportions 30% reworked powder-70% original powder. Samples of the powder blend were then processed by one of the following schemes prior to compaction:

1) As blended
2) Reduced in nitrogen-6% hydrogen at 800°C for 2 hours
3) Blended powder re-hammermilled
4) Re-hammermilled plus reduced in nitrogen-6% hydrogen at 1000°C for 8 hours

When the as blended powder was directly pressed and sintered, the pellets were badly blistered, indicating that the UO_2 might have been oxidized during Spex milling. Reduction treatment of the powder prior to compaction also did not improve the sintering characteristics; similarly, re-hammermilling was not beneficial. The compaction and sintering data for these powders are presented in Table 3.2. Fired densities above 9.75 gm/cc could not be obtained. It is evident that these procedures are inadequate for satisfactory usage of reworked powder. Attempts will be made to use reworked powder by incorporating oxidation-reduction cycles into the procedures. Such cycles have been used with success for improving the sinterability of UO_2, and it is believed that they will correspondingly improve UO_2-PuO_2 powders by lowering the particle size and increasing the surface area.

Phase Relationships in the Pu-O System

(B. Cinai)

During this reporting period, the two phases in the eutectoid microstructure observed after sintering PuO_2 pellets in a nitrogen-6% hydrogen atmosphere or in vacuo were positively identified as PuO_2 and cubic Pu_2O_3.

By heating a pellet with such a two-phase structure in air at 1000 and 1475°C and measuring the gain in weight until no further gain was observed, and knowing the initial amount of both phases, it was possible to calculate the composition of the cubic Pu_2O_3 phase as $PuO_{1.585}$ which is very close to that in the published phase diagram for PuO(i). Assuming that the PuO_2 and $PuO_{1.585}$ in the eutectoid were formed from a single stable phase at the sintering temperature, the composition of the latter was likewise calculated and found to be $PuO_{1.873}$.

(i) Holley, C. E., Mulford, R. N. R., Huber, E. J., Head, E. L., Ellinger, F. H., and Bjorklund, C. W.; Proc. Second Internat. Conf. on the Peaceful Uses of Atomic Energy, Geneva, 1958, vol. 6, pp. 215-220.

Table 3.2

Properties of Reworked Material
UO_2-5 w/o PuO_2

Material	Compacting Pressure TSI	Green Density gm/cc	Fired Density gm/cc	Firing Shrinkage %	Weight Loss on Firing %
As blended	8	6.04	8.20	10.5	1.00
Re-hammermilled	8	6.19	9.23	13.5	1.90
	15	6.45	9.55	12.8	1.00
	23	6.84	9.75	11.6	1.00
Re-hammermilled and reduction	8	6.01	9.40	14.2	0.75
	12	6.33	9.50	13.5	1.60
	16	6.43	9.65	13.0	0.80

Differential thermal analysis has now been carried out on a eutectoid-bearing PuO_2 pellet in an atmosphere of nitrogen-6% hydrogen and has revealed a transformation on heating at 648°C. This value compares with 625 and 654°C obtained previously in an argon atmosphere. It is believed that the average temperature of 642°C for the transformation on heating for these three runs and 650°C on cooling are those of the eutectoid and can be represented by the following reaction:

$$PuO_{2-X} \rightleftharpoons PuO_2 + \alpha\ Pu_2O_3$$

where 2-X can be as low as 1.873. This eutectoid transformation may also be responsible for the anomalous thermal expansion behavior observed by Chikalla(i) in PuO_2 on heating between 600 and 700°C.

Further studies have been made of the effect of sintering atmosphere on the stability of PuO_2. Pellets made by both the oxalate and peroxide routes were sintered for one hour at 1600°C in argon. Metallographic examination revealed a small amount ($< 5\%$) of coherent precipitation in both samples. This was identified in the PuO_2 (made by the peroxide route) as $\alpha\ Pu_2O_3$. PuO_2 pellets, again from oxalate and peroxide sources, were sintered for one hour at 1600°C in air, but only PuO_2 was subsequently observed by both metallography and x-ray diffraction. The effect of moisture in a reducing sintering atmosphere was also investigated. The standard nitrogen-6% hydrogen mixture was bubbled through deionized water and in the process picked up 3.1 w/o mixture. The latter fully prevented the decomposition of PuO_2 pellets made both by the oxalate and peroxide routes on sintering for one hour at 1600°C. It would seem that the presence of a small partial pressure of oxygen at the sintering temperature is sufficient to prevent the decomposition of PuO_2.

The role of residual carbon in the decomposition and fusion of the PuO_2 at 1600°C has also been investigated further. No relationship was found between the tendency for $\alpha\ Pu_2O_3$ formation on sintering and the residual carbon content prior to sintering. This conclusion was reached during investigations with PuO_2 pellets in which the carbon had been varied systematically from about 0.3 to 0% by increasing calcining temperatures. The sintering conditions were one hour at 1600°C in an atmosphere of nitrogen-6% hydrogen. An attempt to obtain further information through the use of theoretically carbon-free PuO_2 (made by the peroxide route) was not fully satisfactory since a carbon content of 0.079% was found after calcination of the peroxide in air at 700°C. This PuO_2 did show a reduced tendency to $\alpha\ Pu_2O_3$ formation, but as the green density of the

---

(i) Chikalla, T. D., Conf. Internat. sur la Metallurgie du Plutonium, Grenoble, 1960, April, Memoire No. 35.

pellets made from this powder was significantly higher (7.6 gm/cc as pressed) than that made under identical pressing conditions from oxalate source material (6.69 gms/cc as pressed), a possibly more rapid sintering of the former material may have allowed less time for its PuO_2 particles to be in contact with the reducing atmosphere.

The residual carbon in the oxalate source PuO_2 has been suspected of being responsible for the traces of fusion occasionally observed metallographically after sintering at 1600°C in the N_2-6% H_2 atmosphere or in vacuo. It is of interest that PuO_2 of zero carbon content showed no fusion even on heating to 1750°C in the N_2-6% H_2 atmosphere, while the PuO_2 made via the peroxide route with 0.079% residual carbon showed a trace of fusion after sintering in a moist N_2-6% H_2 atmosphere at 1600°C. From these observations, it appears that residual carbon in the PuO_2 is associated with the fusion observed on sintering.

It may be conjectured that a plutonium carbide phase is formed, at least temporarily, during sintering and that this phase lowers the melting point of the PuO_2; in fact, an oxycarbide of plutonium similar to that observed in the U-O-C system(i) may be responsible for the observed behavior. To test this hypothesis a carbide mixture was prepared by the deliberate reduction of PuO_2 with graphite at about 1500°C in vacuo. A 50/50 mixture was then prepared using this product and PuO_2 powder having zero carbon content. The resulting mixture was pelletized and sintered for one hour at 1600°C in nitrogen-6% hydrogen. As a control, a carbon-free PuO_2 pellet formed from the same powder batch as that used in the mixture was sintered simultaneously. Subsequent metallographic examination revealed no fusion in the carbon-free PuO_2 pellet but very significant fusion in the pellet formed from the PuO_2-carbide mixture. These results suggest the need for a more intensive study of the phase relationships in the ternary system Pu-O-C.

Evaluation Techniques

(B. Cinai)

A technique has been developed for the cathodic vacuum etching of PuO_2 pellets so that PuO_2, α Pu_2O_3 and grain boundaries can now all be simultaneously revealed. The method is simpler than chemical etching and is certainly superior so far as grain boundary delineation is concerned. Typical photomicrographs at a magnification of X800 and enlarged 25% are shown in Figure 3.1.

(i) EURAEC-1, Progress Report, "Study of Phase Relationships in the U-C-O System", North Carolina State College Contract No. AT(40-1)-2663.

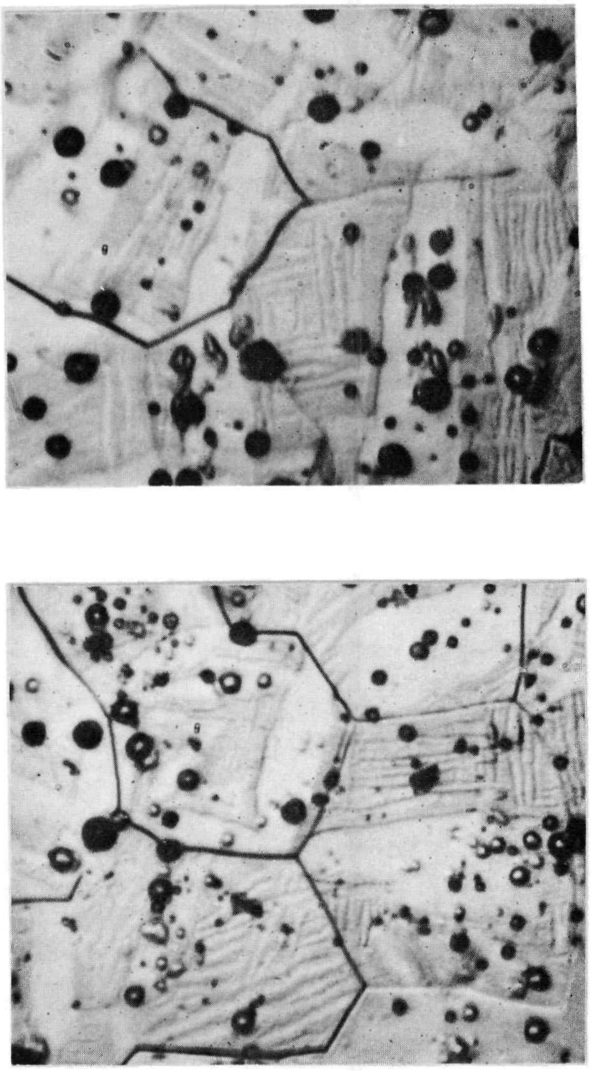

Figure 3.1

Typical Photomicrographs Showing
PuO_2, $PuO_2/\alpha\ Pu_2O_3$ Eutectoid and Grain Boundaries

PuO_2 Pellet No. 63C Sintered for One Hour at 1600°C
in Nitrogen-6% Hydrogen; Polished and Cathodically Vacuum Etched

800X and Enlarged 25%

Thermal Conductivity Experiment
(E. K. Halteman)

The assembly of an apparatus for the measurement of the thermal conductivity of poor conductors at high temperature by the use of point and plane sources is continuing. Little effort has been expended during the quarter since a vendor, Metalizing Industries, Inc., who is fabricating the quartz to metal seals, has experienced difficulties in making these seals vacuum-tight. As a back-up effort, an "O" ring seal has been designed to fit the limited space available. The susceptor blocks are being remachined, and longer quartz tubing obtained to fit the new sealing arrangement. The high voltage supply has been received and is being used to test the high voltage filter sections. The inductances in the filter are being floated at the high potential to reduce winding-to-frame voltage breakdown problems. The electron gun and associated control circuits will soon be tested in a separate vacuum system while the quartz-to-metal seal problem is bypassed or resolved.

FUEL ELEMENT FABRICATION AND EVALUATION

Task 4.00
L. J. Jones

Box and Equipment Installation

(M. Zambernard)

The welding box intended for use in plutonium fuel element fabrication is currently in the final stages of outfitting. This box will be tied to the decontamination box, thus facilitating the removal of welded assemblies from the closed system.

Drawings are currently being prepared to allow enclosing the 8" Stanat Mill in a glove box. The design is such that the box can be evacuated prior to backfilling with an inert atmosphere thereby eliminating a continuous purging sequence. This mill is being set up to develop procedures for the fabrication of dispersion fuel elements, using stainless steel, zircaloy, or any of the refractory metals. Since hot rolling of metals which readily oxidize will be undertaken, it is necessary to make provisions for a good inert atmosphere. Auxiliary equipment being installed includes a muffle-type furnace capable of heating to 1000°C and an infrared heater capable of heating both rolls and tables to 250°C. The heat source for the muffle furnace will be external to the closed system thereby simplifying its maintenance.

A jig for the testing of reaction rates between the ceramic fuel pellets and various cladding materials has been designed and constructed. A thick-walled Inconel tube serves to contain the pellets and the samples of cladding materials in the form of disks sandwiched together. A load of up to 50 lbs can be placed on the samples by a compression spring located at the end of the tube which is normally external to the furnace. This load will apply a maximum pressure of 1000 psi on 0.250 inch diameter pellets. The jig is also equipped to provide any gaseous atmosphere desired. Sandwiches of PuO_2 and UO_2-PuO_2 together with zircaloy, aluminum, and various grades of stainless steel will be subjected to various temperatures up to 1000°C (approximately 600°C for aluminum) in reducing, oxidizing, and inert atmospheres for various periods of time. Upon removal from the jig, the sandwich samples will be sectioned perpendicular to the metal-ceramic interface and metallographically examined for evidence of reaction.

RADIATION TESTING AND EVALUATION

Task 5.00
L. J. Jones

Rabbit Tests
(L. J. Jones, R. M. Horgos)

Fabrication of the samples for short-term irradiations in hydraulic rabbit facilities to determine the relative merits of the various preparation and fabrication procedures has been started. The proposed capsule and fuel element were described previously(1). Each capsule will contain three fuel elements--two containing developmental PuO_2-UO_2 compositions and one containing enriched UO_2 to serve as an in-pile control. Fuel element specifications and operating parameters are given in Table 5.1. The UO_2 control samples have been enriched to produce the same specific heat generation as the PuO_2-UO_2 samples by considering flux suppression and the effective fission cross-sections of the fissile atoms. In the first nine capsules, co-precipitated material and material made by mechanical mixing of the specific oxide components followed by formation of solid solution during the sintering operation will be compared at three burnup rates and hence under three temperature conditions. Attempts will be made to keep the fuel density of these samples identical to allow direct comparison of their in-pile thermal performance (thermal conductivity plus melting point and relative fission gas retention capabilities). Irradiation of capsules 10 through 14 will allow determination of the effect of porosity on the irradiation behavior particularly on fission gas retention. In these capsules, attempts will be made to irradiate all elements at about the same temperature by making allowances for the reduced thermal conductivity associated with the more porous materials.

Stainless steel tubing is being used for both the fuel element cladding and the inner capsule. Assembly of the capsule requires shrinkfitting the stainless steel inner capsule into an aluminum outer capsule. The aluminum capsule components are being machined to match the outside diameter of the stainless steel tubing. The entire capsule assembly, including welding of both inner and outer capsule end plugs and shrinkfitting, is being performed on dummy capsules to develop the necessary techniques.

---

(1) NUMEC P-80, Progress Report, "Development of Plutonium-Bearing Fuel Materials", pages 51 and 52.

Table 5.1

Rabbit Capsule Design Data

Capsule No.	Fuel Element No.	Fuel Composition(1)	Fuel Preparation Route	Fuel Density % Theoretical	Unperturbed Thermal Flux (nv x 10^{-13})	Maximum Fuel Temperature °C	Maximum Clad Temperature °C
1	1-1	Comp. A	Co-precipitated	93-95	7.0	3100	190
	1-2	Comp. D	Co-precipitated	93-95	7.0	3100	190
	1-3	Comp. A	Mechanical Mix	93-95	7.0	3100	190
2	2-1	Comp. A	Co-precipitated	93-95	6.5	2895	180
	2-2	Comp. D	Co-precipitated	93-95	6.5	2895	180
	2-3	Comp. A	Mechanical Mix	93-95	6.5	2895	180
3	3-1	Comp. A	Co-precipitated	93-95	5.5	2470	165
	3-2	Comp. D	Co-precipitated	93-95	5.5	2470	165
	3-3	Comp. A	Mechanical Mix	93-95	5.5	2470	165
4	4-1	Comp. B	Co-precipitated	93-95	7.0	3100	190
	4-2	Comp. D	Co-precipitated	93-95	7.0	3100	190
	4-3	Comp. B	Mechanical Mix	93-95	7.0	3100	190
5	5-1	Comp. B	Co-precipitated	93-95	6.5	2895	180
	5-2	Comp. D	Co-precipitated	93-95	6.5	2895	180
	5-3	Comp. B	Mechanical Mix	93-95	6.5	2895	180
6	6-1	Comp. B	Co-precipitated	93-95	5.5	2470	165
	6-2	Comp. D	Co-precipitated	93-95	5.5	2470	165
	6-3	Comp. B	Mechanical Mix	93-95	5.5	2470	165
7	7-1	Comp. C	Co-precipitated	93-95	4.0	3075	195
	7-2	Comp. E	Co-precipitated	93-95	4.0	3075	195
	7-3	Comp. C	Mechanical Mix	93-95	4.0	3075	195
8	8-1	Comp. C	Co-precipitated	93-95	3.5	2700	175
	8-2	Comp. E	Co-precipitated	93-95	3.5	2700	175
	8-3	Comp. C	Mechanical Mix	93-95	3.5	2700	175
9	9-1	Comp. C	Co-precipitated	93-95	3.0	2335	160
	9-2	Comp. E	Co-precipitated	93-95	3.0	2335	160
	9-3	Comp. C	Mechanical Mix	93-95	3.0	2335	160
10	10-1	Comp. A	Co-ppt or Mech Mix	82-85	5.5	2740	165
	10-2	Comp. D	Co-precipitated	93-95	5.5	2470	165
	10-3	Comp. A	Coppt or Mech Mix	88-91	5.5	2570	165
11	11-1	Comp. A	Co-ppt or Mech Mix	95-97	6.5	2840	180
	11-2	Comp. D	Co-precipitated	93-95	6.5	2895	180
	11-3	Comp. B	Co-ppt or Mech Mix	95-97	6.5	2840	180
12	12-1	Comp. B	Co-ppt or Mech Mix	82-85	5.5	2740	165
	12-2	Comp. D	Co-precipitated	93-95	5.5	2470	165
	12-3	Comp. B	Co-ppt or Mech Mix	88-91	5.5	2570	165
13	13-1	Comp. C	Co-ppt or Mech Mix	82-85	3.0	2595	160
	13-2	Comp. E	Co-precipitated	93-95	3.0	2335	160
	13-3	Comp. C	Co-ppt or Mech Mix	88-91	3.0	2435	160
14	14-1	Comp. C	Co-ppt or Mech Mix	88-91	3.0	2435	160
	14-2	Comp. E	Co-precipitated	93-95	3.0	2335	160
	14-3	Comp. C	Co-ppt or Mech Mix	95-97	3.0	2290	160

(1) Fuel Composition Code
"A" - 0.5 w/o PuO_2 + 7.40 w/o $U^{235}O_2$ + remainder $U^{238}O_2$
"B" - 5 w/o PuO_2 + remainder natural UO_2
"C" - 20 w/o PuO_2 + remainder natural UO_2
"D" - 9.27 w/o $U^{235}O_2$ + remainder $U^{238}O_2$
"E" - 23.95 w/o $U^{235}O_2$ + remainder $U^{238}O_2$

Hot Laboratory Equipment Fabrication
(R. M. Horgos)

Five alpha boxes for the hot cell are being made ready for use. Also, two prototype manipulator boots to facilitate entrance of the manipulators into the sealed alpha boxes are presently being checked for suitability for the remote operations contemplated. In addition, a mechanically driven positioning table to permit entry and removal of the manipulators from the alpha box has been designed and built. This table is made to raise or lower the box with respect to the manipulators. The unit is controlled by a direct drive from the front of the hot cell.

Manipulators for the metallographic cell which were obtained from excess property have been decontaminated and examined to determine the extent of repairs and replacements parts required. These parts have been ordered, and repairs will proceed after delivery of parts. Decontamination of the metallographic steel cell will then be started as soon as the manipulators are operable.

REACTOR PHYSICS AND ENGINEERING PARAMETRIC STUDIES

Task 8.00
K. H. Puechl

Assessment of Plutonium Potential in Near-Thermal Reactors

(J. Ruzbacki)

Two papers having the titles, "The Potential of Plutonium as a Fuel in Near-Thermal Converter Reactors" and "The Potential of Plutonium as a Fuel in Near-Thermal Burner Reactors" will be published in the February 1962 issue of Nuclear Science and Engineering. Since this work was performed, additional studies have been made to determine the sensitivity of the results to changes in the effective cross sections for the various isotopes. Especially the influence of varying degrees of self-shielding in the plutonium-240 isotope is being examined in great detail. The physics portion of this study is essentially completed; assessment of the effect on fuel cycle cost is now underway. Under all reasonable assumptions as to the effective resonance integral of Pu-240, the physics results indicate that high Pu-240 content plutonium is generally an attractive fuel in these near-thermal reactor systems. Specifically, it has been found that the lower the assumed effective absorption cross section of Pu-240, the higher the concentration buildup of this isotope; i.e., the macroscopic absorption in Pu-240 is not a strong function of the assumptions used in determining the effective microscopic cross section. For these reactor systems then, under all reasonable assumptions regarding the Pu-240 absorption cross section, these can always be found a Pu/U concentration range wherein a "negative resistance" effect exists; i.e., wherein the reactivity tends to decrease with further addition of plutonium. Since such ranges were found to exist generally, it may be concluded that relatively long core life (reactivity limiting) is attainable with these systems. The associated economics evaluation which is now underway will offer specific guidance to the materials development program. Specifically, it will allow more accurate determination of Pu/U concentrations of economic interest; it will also indicate the amount and direction of effort that is necessary to achieve the economic benefits associated with a potentially long core life; i.e., it will indicate the effort required to extend the radiation damage limiting life to that inherently possible from physics considerations; further, it will indicate what must be done in the way of materials development to achieve high power densities within the fuel, thereby to lower the high inventory charges associated with the relatively high fuel loadings required for these systems.

Further Development and Modification of the NUSURP Procedure

(W. Ross, J. Ruzbacki)

The NUSURP procedure has now been entirely reprogrammed for the RPC-4000 digital computer. Due to the reprogramming process, many modifications have been included to increase flexibility. A fuel cycle economics program is now being written, so that costs may be determined directly from the physics results without coming off the machine at an intermediate point.

Effort is continuing on the problem related to the discrepancy between experimentally-determined and theoretically-derived values for the U-238 effective resonance integral(1). To date, it has been impossible to obtain a simple expression for the effective resonance integral over the entire range of fuel lump surface to volume ratio and extraneous potential scattering that forces agreement between experimentally-determined and theoretically-derived cadmium ratio data.

(i) NUMEC P-80, Progress Report, "Development of Plutonium-Bearing Fuel Materials", page 54.

PREPARATION AND COATING OF SPHERICAL OXIDE PARTICLES

Task 11.00

C. S. Caldwell L. J. Jones

Production of Spherical PuO_2 by Plasma Torch

(R. M. Horgos, J. Miles)

Prior to committing the plasma torch to PuO_2 operations, a considerable number of runs on UO_2 were satisfactorily completed. The yield of spherical particles in a pre-chosen size range (-80 +120 mesh) was approximately 70% of the initial feed material. These runs verified the conclusions reached in prior UO_2 runs(i); namely, (1) a small amount of hydrogen addition to the inert gas is required to prevent superficial surface oxidation of the UO_2, (2) completely spherical particles having a smooth fire-polished surface are produced from both crushed high-fired UO_2 pellets and high-fired UO_2 spherical particles, and (3) a void is found at the center of most of the resultant UO_2 spheres.

Immediately following the completion of these UO_2 studies, the plasma torch and its glove box were committed to plutonium. The initial trials on PuO_2 indicated that the torch parameters which were optimum for UO_2 were unsatisfactory for PuO_2. On the first two runs using PuO_2 the flame temperature was too high, thereby resulting in very poor yield, presumably from vaporization of the PuO_2. On the third run the flame temperature was decreased considerably and resulted in incomplete melting; however, the particles which did melt were spheroidized and decreased in size from 80 to 400 mesh. Additional trials under similar conditions resulted in the severe decrease in particle size. In addition, the range of particle size varied considerably within one batch with some particles being about 5 to 7 times larger than the smallest. However, all melted particles were definitely spherical, and the surfaces bright and shiny. Following these runs, it was concluded that the size change was either due to the poor thermal shock resistance of PuO_2 or due to insufficiently large feed material. There was also some evidence that the particles were being reduced in size by the torch screw-feed mechanism before reaching the plasma. Therefore, emphasis was given to modifying the existing feed mechanism and torch nozzle to permit acceptance of larger feed material and to remove the source of mechanical comminution. The feed mechanism was, therefore, converted to a vibration-type device

---

(i) NUMEC P-70, Progress Report. "Development of Plutonium-Bearing Fuel Materials", page 38.

with a variable aperature to control feed rates. With these modifications, particles having a maximum size of 20 mesh can be fed through the torch.

In addition to the equipment modifications, extreme variations in the torch operating parameters have also been tried. In general, optimum conditions were found to consist of lowest possible plasma gas flow (30 ft^3/hr) and relatively high carrier gas flow (30 ft^3/hr). Using argon and a torch power input of 800 amps, the calculated temperature of the plasma is 22,000°F under these conditions.

It is not to be inferred that the particles also reach this temperature. Rather, when using the plasma torch for the spheroidization of particles, an important parameter appears to be the local aerodynamic condition present at the plasma flame since any gas barrier must be overcome by the kinetic energy of the particle as it enters the plasma stream. The depth into the plasma flame cone reached by the particle and its dwell time in the plasma determine the maximum temperature of the particle.

Under the foregoing operating parameters, satisfactory spheres of PuO_2 were obtained from the following feed material: (1) partially-sintered PuO_2 spheres fired at 1475°C having a size range of -80 +115 mesh, and (2) crushed high-fired PuO_2 pellets having a size range of -60 +80 mesh. A relatively good yield of -70 +120 mesh particles resulted from both feed materials; the product produced from crushed pellet feed is shown in Figure 11.1. Cross-sectional structures at 100 and 200X of the spheres formed from partially-sintered PuO_2 spheres are shown in Figure 11.2 (a and b). Note the appearance of a porous non-fused core in most of these spheres. Apparently, the plasma tended to fire-polish the surface of these spheres without completely fusing the particles. Cross-sectional structures at 100 and 200X of the spheres formed from crushed high-fired PuO_2 pellets are shown in Figure 11.3 (a and b). Herein, note that all sharp angular surface characteristics of crushed material have disappeared and that most of the spheres possess the central voids characteristic of low conductivity ceramic particles which have been fused.

During the next report period, the optimum torch conditions for preparation of spheres from sintered agglomerates and pre-shaped spheres will be systematically obtained, since the use of crushed high-fired pellets as feed appears to be costly.

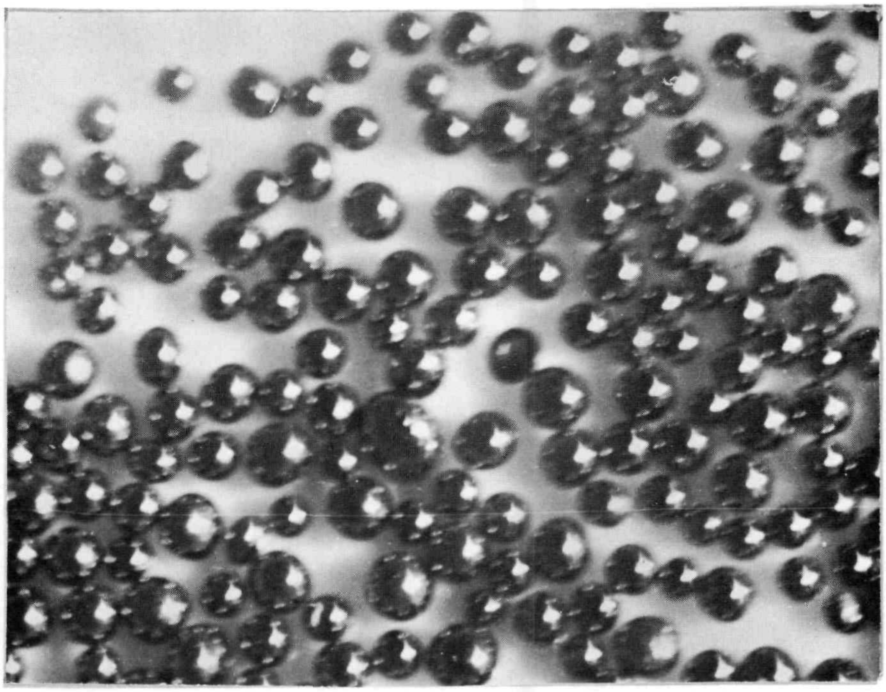

Figure 11.1

PuO_2 Spheres Produced
from Crushed High-Fired Pellets

20X Enlarged 4 Times

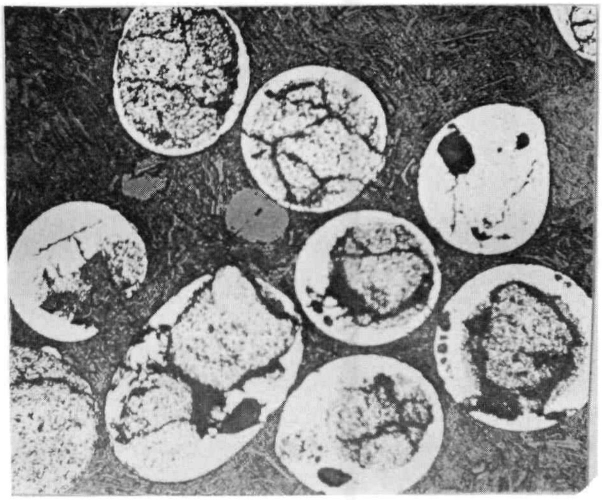

(a) 100X

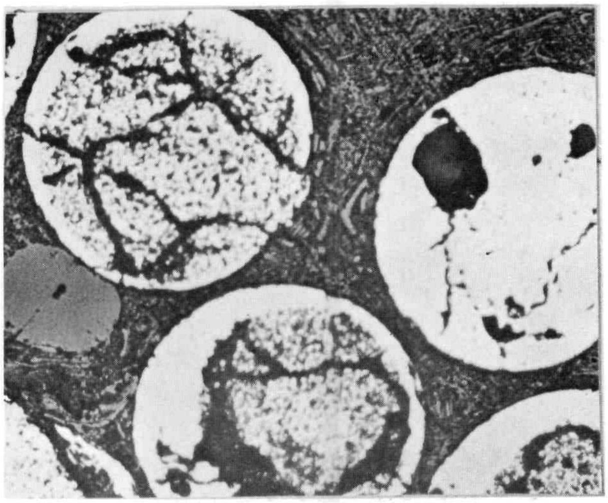

(b) 200X

Figure 11.2

PuO_2 Spheres Produced by Plasma Torch from Spherical Feed Material Fired at 1475°C

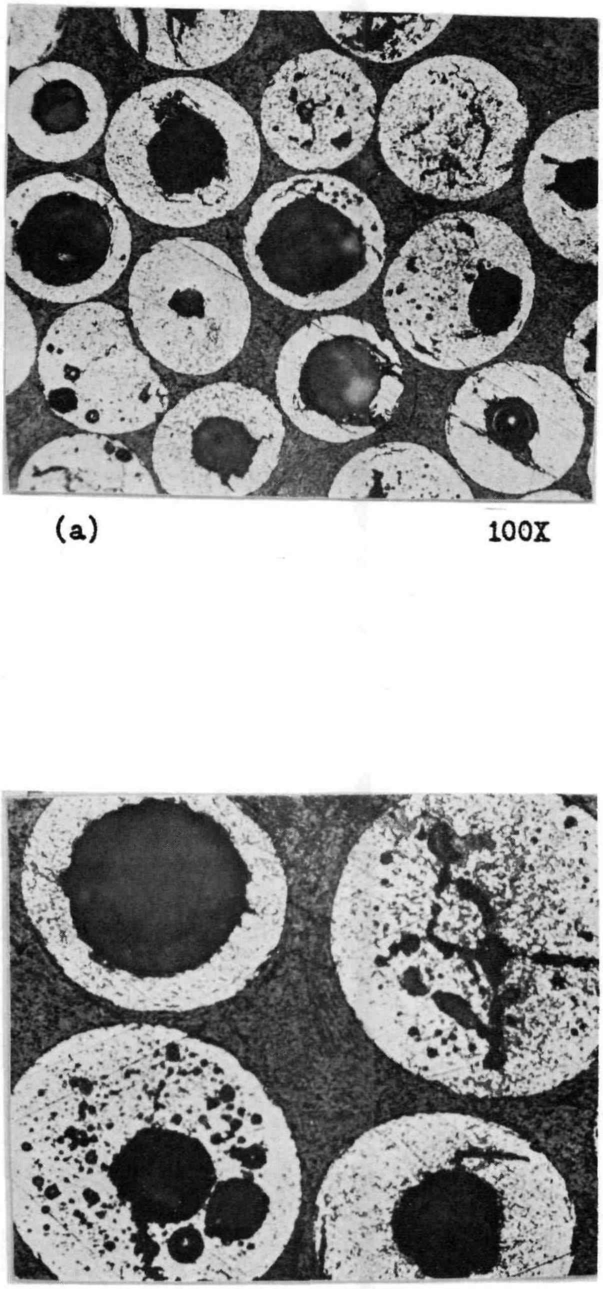

(a) 100X

(b) 200

Figure 11.3

PuO_2 Spheres Produced by Plasma Torch from Crushed High-Fired Pellet Feed

Preparation of Spherical PuO_2 Particles From Ceramic-Grade Powders

(C. S. Caldwell, A. Biancheria, J. Miles)

In addition to plasma torch spheroidization, a multi-step process of dry-pressing, granulation, sizing, shaping, and sintering has also been used successfully to yield a nearly-spherical product, controllable within one mesh size, over the range 80 to 170 mesh (U. S. Series).

Starting with virgin PuO_2 powder of intermediate surface area, wafers were dry-pressed in a one-half inch diameter double acting die at pressures of 2-4 TSI. Breakup of wafers on successively smaller screens, beginning with 10 mesh, was carried out manually. Once reduced to the approximate green size required, based on a green wafer density of approximately 5 gm/cc, the granular material was agitated in contact with a screen to produce nearly-spherical shapes. Undersize material was broken up to a fine powder and recycled through the process. The shaped material was pre-sintered at temperatures of 1000 or 1200°C, re-screened, then sintered to final density at temperatures in the range 1350-1600°C for 4 hours. A platinum-10% rhodium wound furnace (air atmosphere) was used for these operations. Off-size, out-of-shape, and agglomerated particles were subsequently removed by screening. Typical metallographic sections of particles produced by the above route are shown in Figures 11.4 through 11.9. These represent material formed at a green density of 5 gm/cc and sintered at 1350, 1400, and 1475°C. It is clear that incomplete sintering has occurred in a number of the particles shown. It is expected that improved sintered density can be obtained at higher temperatures with the use of a reducing atmosphere and/or controlled moisture content. This effect will be checked in the near future.

In addition to forming green particles by size reduction, it was found that some PuO_2 powders tended to agglomerate into near-spherical shapes during agitation. On-size material made in this manner was combined with material made by the main process. Particles formed in this manner can be readily identified by their appearance as sectioned since two zones exist with each having different sintered density. Uniform density can probably be attained by permitting agglomeration to start with very small original nuclei; however, the green density of such particles will be low, and higher sintering temperatures may be required. In any case, the work to date indicates that extremely close control of powder characteristics is required. Powder surface area, although an important factor in fabricability is not the only controlling variable. Particle morphology, size distribution, and preparation history are apparently all related to formability. For example, spheres could not be produced from over-calcined PuO_2, or PuO_2 made from dilute plutonium nitrate by the oxalate process.

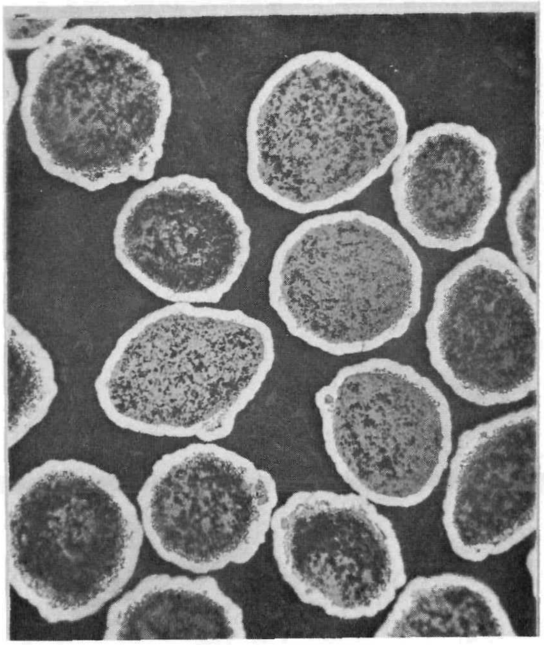

Figure 11.4

Spheroidized PuO_2,
Sintered at 1350°C,
with 10-15 micron Nickel Coating

(100X) Sample C

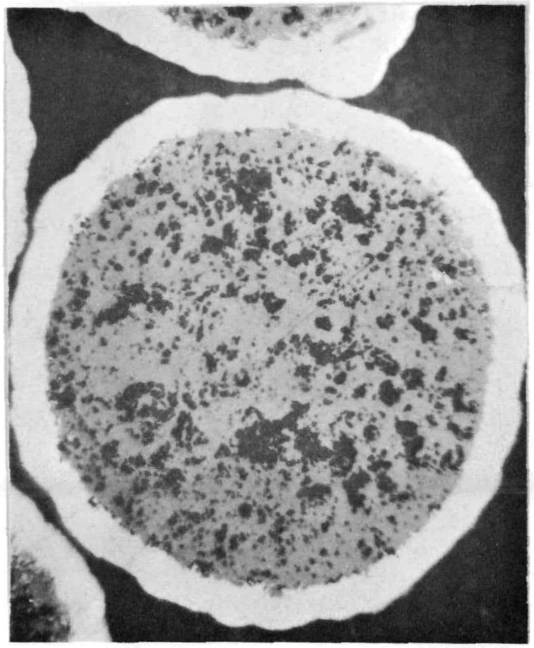

Figure 11.5

High Magnification Cross-Section
of Spherical PuO_2,
Sintered at 1350°C,
with 12 micron Nickel Coating

(400X) Sample C

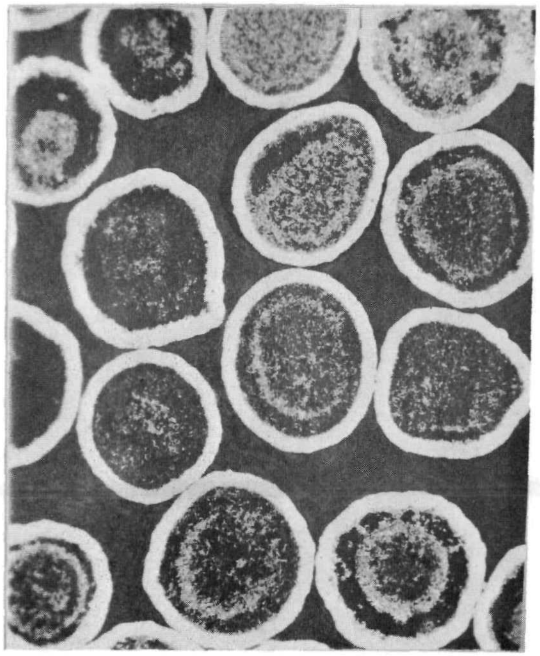

Figure 11.6

Spheroidized PuO_2,
Sintered at 1400°C,
with 20 micron Nickel Coating,
Showing Two Zones of Sintering
Due to Non-Uniformity
in Green Spheres

(100X) Sample DE

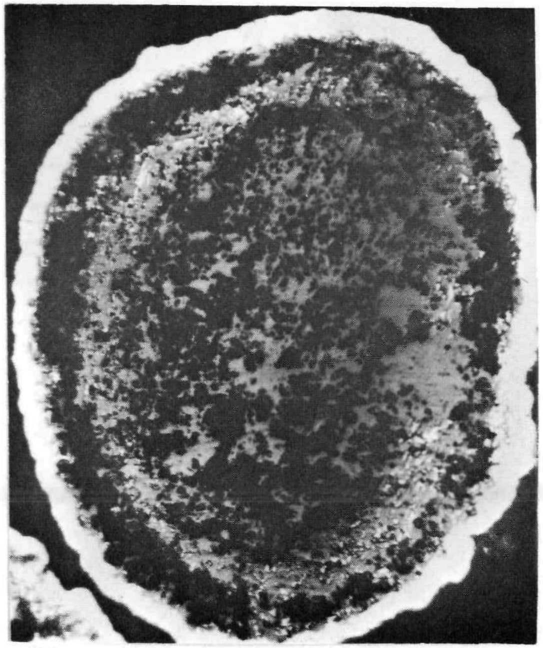

Figure 11.7

High-Magnification Cross-Section
of Spherical PuO_2,
Sintered at 1400°C,
Showing Penetration of Nickel
Coating Within Partially-
Sintered Zones

(400X) Sample D

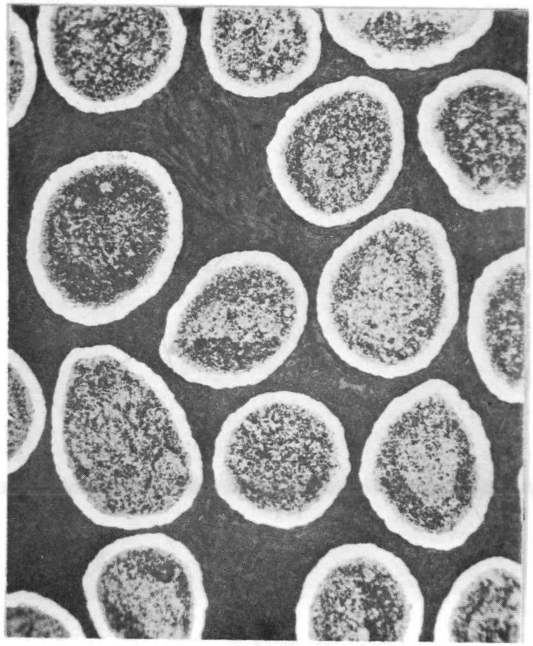

Figure 11.8

Spheroidized PuO_2,
Sintered at 1475°C,
with 15-20 micron Nickel Coating

(100X) Sample E

Figure 11.9

High-Magnification Cross-Section
of Spherical PuO_2, with 10 micron
Electrolytic Copper Coating
Over 3-4 micron Nickel Base Coat

(400X) Sample E

Application of Nickel and Copper Coatings to Spherical PuO_2

(J. Miles, R. Recchia, F. Shipko)

In order to evaluate the feasibility of coating spherical PuO_2 particles fabricated by the granulation process, spherical material (-80 +100 mesh) sintered at 1350, 1400, and 1475°C was coated as follows:

1) Multi-stage "electroless" nickel coating up to 20 microns thickness.
2) Electrolytic copper up to 15 microns thickness applied over a 2-4 micron "electroless" nickel base coat.
3) Electrolytic copper applied over a vacuum evaporated 1-3 micron copper base coat.

Methods (1) and (2) were successful; however, method (c) was discarded after four unsuccessful attempts. In this case, the thin copper base layer was evidently attacked by the copper cyanide plating solution before sufficient thickness of electrolytic copper had time to deposit and thus protect the underlying layer. Substrate (surface) roughness probably contributed to the vulnerability of the base conducting layer.

Method (1) utilized a standard nickel chloride-hypophosphite bath(i), manually agitated, operating at 80-85°C. Teflon containers were used. Mechanical agitation and thermostatic temperature control were used successfully in prototype UO_2 coating trials; however, such improvements in process control were not made during this preliminary work with PuO_2. Inferior quality sintered particles occasionally exhibited penetration by the nickel (Figure 11.7) but in general even partially sintered material was adaptable to coating by this method with little, if any, penetration. Coating thickness control was achieved by exposure time, bath concentration, and temperature. Since starting material for these early runs was purposely allowed to contain a moderate percentage of off-grade, odd-shape, partially densified particles in order to determine coating effectiveness under severe conditions, thickness control could only be maintained within ±15%. Coating process control was observed to be similar to past experience with UO_2; a slight acceleration in coating rate, possibly due to radiation effects, was the only significant difference. Based on experience to date, coating control, and uniformity on plasma-melted spherical material should permit thickness control within ±5% or better.

(i) NUMEC-NYO-2801, Final Report on Contract AT(30-1)-2354.

Method (2) utilized a miniature rotating barrel plater for agitation during electrodeposition. Standard copper cyanide plating bath formulations were used(1), and contact between the platinum wire cathode and charge was maintained by the use of larger 20 mesh copper-plated steel shot. The large diameter shot also served to improve agitation. The metallographic section in Figure 11.9 shows that uniform bonding and coating thickness were obtained using this process. Several process deficiencies were isolated and corrected during the coating of three grades of spherical material sintered at 1350, 1400, and 1475°C. Control of D.C. current tended to be erratic due to the physical arrangement of the cathode wire, and possible gas blanketing. Also, agglomeration losses were high in several runs due to inadequate particle motion in the vicinity of the cathode wire; i.e., clumps of particles appeared to cement together and form a "grape-cluster" which could not be broken up physically. To remedy these situations, a higher ratio of dead shot to charge was used in addition to a higher bath temperature. One major disadvantage of the process was the slow coating rate (approximately 1 micron/hour); however, potential for improvement exists, and the process can be extended to other electrolytic deposition schemes with only minor modifications.

Method (3) utilized vacuum evaporation to form the base coating of copper (1-3 microns) on 150 micron PuO_2 spheres prior to electroplating. An oversize spiral tungsten filament was arranged to hold the required amount of copper for evaporation vertically downwards onto the charge. The bare PuO_2 particle charge (~ 3 gms) was separated out in a thin layer on a circular pan beneath the filament and the charge was vibration-agitated during evaporation to provide uniform exposure to all surfaces. The resultant coating was examined microscopically and was observed to have 100% coverage, although the external surface was somewhat pebbly, reflecting the surface condition of the substrate itself. Although useful only for small quantities of material, the vacuum-evaporation method can be extended to many metallic and non-metallic coatings of interest, particularly where a high-purity coating is required, or where special enviornmental conditions prohibit the use of other coating processes.

(i) Metal Finishing, (1960), published by Metal Digest.